



# Nanotechnology based therapeutic application in cancer diagnosis and therapy

Ragini Singh<sup>1</sup>

Received: 23 July 2019 / Accepted: 3 October 2019 / Published online: 23 October 2019  
© King Abdulaziz City for Science and Technology 2019

## Abstract

Due to the lack of early diagnosis, cancer remains as one of the leading cause of human mortality. Inability to translate research into clinical trials and also inability of chemotherapeutics delivery to targeted tumor sites are major drawbacks in cancer therapeutics. With the emergence of nanomedicine, several nanoprobosc (conjugated with targeting ligands and chemotherapeutic drugs) are developed. It can interact with biological system and thus sense and monitor the biological events with high efficiency and accuracy along with therapy application. Nanoparticles like gold and iron oxide are frequently used in the computed tomography and magnetic resonance imaging applications, respectively. Moreover, enzymatic activity of gold and iron oxide nanoparticles enables the visible colorimetric diagnostic of cancer cells, whereas, fluorescence property of quantum dots and upconversion nanoparticles helps in *in vivo* imaging application. Other than this, drug conjugation with nanoparticles also reduces the systemic toxic effect of chemotherapeutic drugs. Due to their several unique intrinsic properties, nanoparticles itself can also be employed as therapeutics in cancer treatment by photothermal therapy (PTT) and photodynamic therapy (PDT). Thus, the main focus of this review is to emphasize on current progress in diagnostic and therapeutic application of nanoprobosc in cancer.

**Keywords** Theranostic · Nanoparticles · Drug delivery · Cancer · Tumor biomarkers

## Introduction

According to the World Health Organization (WHO) report, in 2018 cancer causes the death of 9.6 million people and is the second most death causing disease, globally. It has also been estimated that at global level, 1 in 6 death is caused due to cancer (WHO 2018). International Agency for Research on Cancer estimates that by 2030 this data will reach to 22.2 million new cases and about 13.2 million death (Bray et al. 2012). Cancer can be cured successfully if diagnosed initially, as according to WHO report also, 30% of people could have been saved if their cancer was detected at an early stage (Perfezou et al. 2012). Likewise, in the case of breast cancer, patient's 5-year survival rate is estimated to be 85% if diagnosed at stage 0 and I, it decreases to 85% in stage II diagnosis and only 20% of patients can survive if diagnosed at stage IV (Chen et al. 2013). In a current

scenario, several reports are available which illustrates about recent progresses in deciphering cancer at molecular level, but there is lack of reciprocity in translation of these reports into clinical trials. There are principally two main hurdles in cancer therapy i.e. diagnosis of cancer at an advanced stage and inability to deliver therapeutic chemicals to targeted tumor site without consequent damage to healthy cells (Cryer and Thorley 2019). Earlier, immunological work by Paul Ehrlich's defines the "Magic bullet" paradigm which allows the selective delivery of therapeutics to cancer cells at its very early stage (Strebhardt and Ullrich 2008). With the advancement of proteomics, genomics, and nanotechnology, this proposed concept can be proved to be real. With the help of these techniques, researchers have identified several biomarkers associated with tumorigenesis and progression (Nakamura and Nishimura 2017; Shindo et al. 2019). Additionally, new screening technology also agrees with the identification of peptide sequences, antibodies and nucleic acid aptamers with high affinity towards cancer specific biomarkers (Stambuk et al. 2019; Chen et al. 2017a; Shepard et al. 2017).

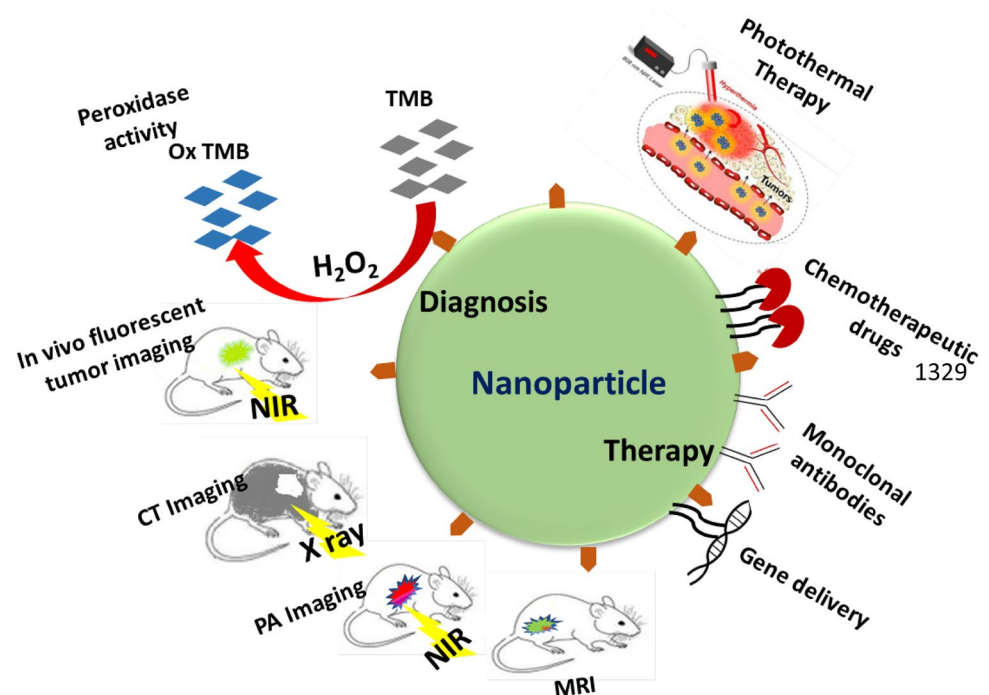
✉ Ragini Singh  
singh@lcu.edu.cn

<sup>1</sup> School of Agriculture Science, Liaocheng University, No. 1 Hunan Road, Liaocheng, Shandong, China

Nanotechnology is a multidisciplinary science consisting of biochemistry, physics and material science, and has found a wide range of applications in biomedicine field. It generally defined as fabrication and application of the man-made material i.e. nanomaterials (NMs) (size range of 1–100 nm) in targeted drug delivery, biosensing, imaging, photothermal therapy (PTT), photodynamic therapy (PDT) etc. (Chen et al. 2019; Kim et al. 2019; Yang et al. 2019; Poonia et al. 2017). Nanoparticle (NP) is a wide term used to define different shapes and sizes of nanovector structure which exhibit unique physicochemical properties. Thus, by utilizing their unique properties, NPs have ability to revolutionize the way in which many diseases like cancer are currently diagnosed and treated (Cryer and Thorley 2019; Chen et al. 2013). Several nanoprobe coupled with respective ligands and chemotherapeutic drugs have been developed which can interact with biological systems and thus can sense and monitor biological events with high efficiency along with therapy application (Fig. 1). In *in vivo* execution, these nanoprobe are administered and accumulated at tumor site by ligand-biomarker interaction to produce signals for diagnosis purpose. Furthermore, due to their intrinsic property the accumulated NPs can also be employed in cancer therapy by PTT, PDT. It is also equally beneficial in *in vitro* analysis of urine, blood, saliva, and tears. NPs can afford such potential due to their high surface to volume ratio, magnetic and electrical properties, diversity of shape and size either solid or hollow, desirable chemical composition with preferred surface chemistry (Cryer and Thorley 2019). Within human body also, NPs have potential

to overcome the chemical and biological barriers allowing for augmented diagnosis and therapy with higher biocompatibility and low invasiveness. However, despite all these benefits, promising results of pre-clinical trials cannot be entirely deciphered into real life scenarios. This is primarily due to the challenges associated with its large scale synthesis, reproducibility, toxicology behavior and inaccurately evaluated safety hazards. Long term safety assessment of NPs needs to be primarily evaluated as it can induce toxicity if used for longer period, such as bio-persistent and elongated use of NPs in pre-clinical trials for pulmonary drug delivery induces fibrosis in hypertensive rats (Wang et al. 2013b). Moreover, *in vivo* studies on mouse showed that intranasal delivery of copper oxide (CuO) NPs induces pulmonary toxicity and fibrosis in lung tissues (Lai et al. 2018). Apart from the toxic hazardous effect, several NPs possess intrinsic enzyme mimetic and fluorescence properties, which allows them to be preferably utilized in diagnosis and treatment of various disease including cancer. NPs like gold NPs (AuNPs) and iron oxide (IONPs) are well known to possess peroxidase mimetic activity and thus can be used for visual detection of cancer cells as well as in therapy. Peroxidase-like activity of NPs catalyzes the decomposition of hydrogen peroxide ( $H_2O_2$ ) to produce hydroxyl radical ( $\cdot OH$ ) which leads to cytotoxic effect in cancer cells (Fu et al. 2017; Maji et al. 2015). Quantum dots (QDs) on the other hand offers great advantage over traditional organic fluorescent dyes and can be employed in cancer molecular imaging and targeted therapy. Additionally, fluorescence of quantum dots (QDs) and upconversion NPs (UCNPs) upon near-infrared (NIR)

**Fig. 1** Schematic showing various applications of nanoparticles in diagnosis and therapy of cancer



activation enables their detection in deep tissues which make them appropriate for in vivo imaging with high signal to background ratio (Li et al. 2019a; Fang et al. 2016).

The main focus of this article is to review the current diagnostic and therapeutic application of nanotechnology in cancer. First, a brief description of tumor associated biomarkers is provided followed by a discussion regarding the design and fabrication of AuNPs, IONPs, QDs and UCNPs based cancer diagnosis techniques. The future advancement of nanotechnology is also emphasized in more wide application.

## Tumor biomarkers

Tumor biomarkers are generally proteins, which can be elevated in cancerous cells in response to altered molecular conditions. It can be found in blood, saliva, urine or tissue of the cancer patients. These biomarkers are classified into three categories based on their location i.e. extracellular, intracellular and one found on cell membrane. Table 1 summarizes the common cancer biomarkers which are well studied and plays an important role in NPs based diagnostic system.

### Liver cancer

Alpha-fetoprotein (AFP) is the most commonly used liver cancer serum biomarker and found to be overexpressed in 80–90% of cases. In liver cancer, AFP overexpression is caused mainly due to the hypermethylation and thus silencing of ZHX2 (zinc-fingers and homeoboxes 2, repressor) (Liu et al. 2015). Evaluation of proteoglycans, enzymes, isoenzymes, oncofetal antigens, versican, and glypican3 also helps in the early detection of liver cancer. Sorafenib, drug used in liver cancer treatment shows improved response with low neutrophil to lymphocyte ratio, high s-c-kit, vascular endothelial growth factor (VEGF-A) amplification, low hepatocyte growth factor and extra-hepatic growth (Galle et al. 2019).

### Breast cancer

Monitoring of molecular biology characteristic of breast cancer originates several biomarkers which are well engaged in therapeutic studies like human epidermal growth receptor (HER2), phosphatidylinositol 3-kinase, cyclin-dependent kinases (CDKs) and insulin-like growth factor 1 receptor (Weaver and Leung 2018). HER2 found to be overexpressed in nearly 15–20% of newly diagnosed breast cancer and also associated with the aggressiveness of cancerous cells. Trastuzumab is a widely used chemotherapeutic agent in targeting HER2, it binds to the juxtamembrane portion of HER2 extracellular

domain and blocks the activation of intrinsic tyrosine kinase which further limits the signaling pathways and thus cell proliferation (Dean 2015). Additionally, high blood level of CA 15-3 (cancer antigen 15-3) is also seen in < 10% of patients in the early stage of breast cancer and around 70% patients in advanced stage of breast cancer (Akram et al. 2017).

### Lung cancer

Advancement in understanding lung cancer at a molecular level leads to the identification of various cancer biomarkers. Anaplastic lymphoma kinase (ALK), epidermal growth factor receptor (EGFR) and HER2 are different tyrosine kinase receptors frequently overexpressed in nearly 62%, 3.7–7% and 7–34.9% of non-small lung cell carcinoma (NSCLC), respectively. ROS proto-oncogene 1, receptor tyrosine kinase (ROS1) is another tyrosine kinase receptor belongs to the insulin receptor family and expressed in 1–2% of NSCLC. Several other lung cancer biomarkers are fibroblast growth factor receptor (FGFR), Kristen rat sarcoma viral oncogene homolog (KRAS), RET and MET proto-oncogenes, phosphatidylinositol-4,5-bisphosphate 3-kinase catalytic subunit alpha (PIK3CA) and neurotrophic receptor tyrosine kinase 1 (NTRK1). Gefitinib, afatinib and erlotinib are frequently used tyrosine kinase inhibitors used in the treatment of NSCLC (Villalobos and Wistuba 2017).

### Colorectal cancer

EGFR serves as a key target in colorectal cancer treatment as it governs the major signaling pathways of cancer cells i.e. proliferation, migration, adhesion, angiogenesis, and survival (Pucci and Lauriola 2019). Cetuximab and panitumumab are Food and Drug Administration (FDA) approved drugs, frequently used in treatment of colorectal cancer. These drugs bind to the extracellular domain of EGFR and thus down-regulate the prooncogenic signaling. Another biomarker for colorectal cancer is oncogene BRAF and its mutation is reported in nearly 8–12% cases, with most common mutation is V600E (Yiu and Yiu 2016). Preclinical trials demonstrated that inhibition of BRAF may induce the EGFR expression. Additionally, HER2 amplification has also been reported in nearly 2–11% of metastatic colorectal cancer, found to be more common in left-sided colon and rectal tumor and also thought to provide resistance to EGFR-targeted chemotherapy (Piawah and Venook 2019).

## Gold nanoparticles

Gold nanoparticles (AuNPs) are significantly employed as a cancer theranostic agent due to their physical properties and tailored surface functionalization. Its unique optical

**Table 1** Various cancer related biomarkers and their expression in various cancers

Biomarkers	Description	Inhibitors	References
EGFR and HER2	EGFR is a protein found in the membrane of several types of cancers. Its mutation is mainly associated with autonomous cell growth, apoptosis inhibition, and metastases. It belongs to tyrosine kinase family i.e. HER family. Binding EGFR as dimers either with itself or HER2 will further stimulate protein-tyrosine kinase and activate the intracellular protein tyrosine kinase	Cetuximab, zalutumumab, matuzumab, pertuzumab	Chen et al. (2013); Sebastian et al. (2006); Casalini et al. (2004)
VEGF receptor (VEGFR)	VEGF belongs to the growth factor family and plays a crucial role in angiogenesis (employed in tumor progression). To inhibit the VEGF-VEGFR interaction one approach is to sequester VEGF with antibody and second is to block VEGFR	Bevacizumab, IMC-1C11, IMC-1121B and CDP791	Ferrara (2002); Youssoufian et al. (2007); Chen et al. (2013)
Folate receptor (FR)	FR has been found to be overexpressed in many cancers mainly ovarian and endometrial cancers. Folic acid binds to cancer cells 20 times more than normal epithelial cells	Farletuzumab, vintafolide	Chen et al. (2013); Weitman et al. (1992); Marchetti et al. (2014); Cheung et al. (2016)
Prostate-specific membrane antigen (PSMA)	PSMA is a transmembrane glycoprotein, expressed moderately in hyperplastic and benign prostates but highly up regulated in malignant tissues. Its increased expression is related to tumor aggressiveness and also found to be overexpressed in non-prostatic tumors like colon, breast, and lung	7E1, J591, MDX-070, BIND-014	Israeli et al. (1993); Olson et al. (2007); Chen et al. (2013)
Phosphatidylserine (PS)	In normal cells, PS flattened on the cytosolic side whereas, in apoptotic cells, it flipped to the outer side. Its high level is found in tumor vascular endothelium	Phosphatidylcholine-stearylamine (PC-SA)	Verhoven et al. (1995); Chen et al. (2013); De et al. (2018)
Integrins	Integrins belong to the family of cell adhesion molecules. Plays crucial role in tumor angiogenesis. Particularly, integrin $\alpha_v\beta_3$ is widely studied as tumor biomarker and efficiently binds to arginine-glycine-aspartic acid (RGD)	Volociximab, Intetumumab, LM609	Hynes (2002); Kobayashi et al. (2017); Chen et al. (2013)
Matrix metalloproteinase (MMP)	MMP belongs to zinc-dependent endopeptidases family and able to degrade component of extracellular matrix (ECM). Its activation is associated with tumor. MMP2 high expression is found in breast cancer cells	Peptide sequence, HWKHLHNTKFTL, short target peptide, CTTHWGFTLC.	Chen et al. (2013); Scherer et al. (2008)

property, make them suitable for NIR-active imaging probe for cancer detection and therapy (Guo et al. 2017). In addition to this, AuNPs also serves as a suitable candidate for selective cancer targeting due to their easy functionalization with active ligands at 100-fold higher density than conventional liposomes (Fernandes et al. 2017). Recently, Farooq et al. reported the efficient AuNPs based dual drug i.e. bleomycin (BLM) and doxorubicin (DOX), delivery system to cervical cancer (HeLa) cells (Farooq et al. 2018). The proposed system has several advantages like specific cancer cells environment mediated drug release, high stability, and loading capacity as well as enhanced cellular uptake in HeLa cells. Another major advantage of this study is combination of two drugs (acts by different mechanisms) at single platform which can overcome the drug-resistant risk of cancer cells. Other than the therapeutic agents, gene therapy has also created new avenue in treatment of several genetic disorders including cancer, with good safety profiles and transient tolerable toxicities (Mbatha and Singh 2019; Amer 2014). In this context, Mbatha et al. synthesized the folic acid (FA) and poly(amidoamine) (PAMAM) grafted AuNPs and demonstrated the targeted delivery of plasmid containing luciferase gene (pCMV-*Luc*DNA) to various cancer cells in vitro by using as-prepared AuNPs containing nanocomplex (Mbatha and Singh 2019). FA modified AuNPs shows receptor-mediated internalization into folate receptor (FR) expressing cells which further increases the expression of transgenes. Here, synthesized nanocomplex offers an advantage to protect the plasmid from serum nuclease degradation activity. As this nanocomplex can be well tolerated by different cell lines, it can be effectively utilized in transfection purpose. Peptide-drug-conjugates (PDC) is another approach for specific drug delivery application which can reverse drug resistance and also can deliver multidrug payloads (Gellerman et al. 2013; Kalimuthu et al. 2018). A major drawback in use of PDC for drug delivery application is its low stability due to enzymatic hydrolysis action in blood, liver, and kidney (Du and Stenzel 2014). To overcome this problem, PDC can be conjugated to NPs which improve its pharmacodynamics and pharmacokinetics during drug delivery process (Perez-Ortiz et al. 2017). In this context, Kalimuthu et al. demonstrated that the AuNPs conjugation can stabilize PDC and also ameliorate its drug delivery efficiency and bioavailability, as plasma half-life of AuNPs seems to be more than that of PDC (Kalimuthu et al. 2018). As reported, half-life of PDC alone is in the range of 10.6–15.4 min, however, upon AuNPs conjugation its half-life increases significantly to 21.0–22.3 h. Another advantage of AuNPs conjugation is retained toxicity of PDC, as PDC alone loses its toxic effect after 24 h pre-incubation, however upon AuNPs conjugation it retains its toxic effect even after 72 h of incubation. AuNPs ability to extend the bioavailability of PDC may circumvent the penetration requirement

of NPs into tumor cells, which is major hurdle in application of some NPs. Improved stability of PDC upon AuNPs conjugation led to the develop slow-release formulations of PDC comprising targeted drug delivery system. Other than AuNPs, gold nanocluster (AuNCs) is another well-known NM which can be used in cancer diagnosis and therapy due to strong NIR absorption which makes them a potential candidate in hyperthermia based cancer therapy. Additionally, AuNCs assembly of small size AuNPs (> 6 nm) can be dissociated into single unit and can be excreted out from body which also minimizes the chance of side-effects (Deng et al. 2015; Lee et al. 2018). Recently, Lee et al. demonstrated the albumin-polyallylamine AuNCs (BSA/PAH-AuNCs) with high absorption capacity which is beneficial for surface plasmon based hyperthermia (Fig. 2) (Lee et al. 2018). Here, albumin plays a crucial role of stabilizer and surfactant in synthesis of loosely associated large aggregates which produces small AuNCs with slight negative charge, upon sonication. These AuNCs exhibit excellent hyperthermal effect (~ 60 °C) at ~ 808 nm NIR laser irradiation and shows remarkable toxicity to breast cancer (4T1) cells in vitro and their tumor xenografts in vivo which indicate their remarkable capacity to inhibit the breast cancer growth with negligible toxic effect in histology. As shown in Fig. 2, large Au nano-aggregates are formed due to interaction between negatively charged AuNPs and positively charged PAH. Further, it can be broken into small AuNCs by sonication in presence of BSA, as stabilizer. AuNCs here shows localized surface plasmon resonance (LSPR) in response to NIR of 808 nm wavelength. Upon irradiation its temperature increases up to 10 min in comparison of AuNPs and PBS tested, simultaneously. As shown in Fig. 2, BSA/PAH-AuNCs are localized in the tumor site of 4T1 xenografted nude mice, and its temperature increases to 55 °C in 5 min upon 808 nm NIR irradiation, which is well enough for hyperthermia effect. These complexes are found to be very stable until circulated in blood, as it reaches the tumor site, NIR irradiation facilitates its disassembly into smaller units. Breakdown of complex into smaller particles also reduces the possible toxicity in body as it can be easily filtered via kidney (Fig. 2). Linking of drugs to NPs surface requires several steps like NPs synthesis, its surface functionalization with biocompatible polymers followed by drug conjugation. However, mostly used processes are complicated and also used harsh chemical which enhances the toxicity of drugs. To overcome these problems, several researchers have reported the one-pot easy synthesis of drug coated NPs (Plan Sangnier et al. 2018; Chaudhary et al. 2015). Sangnier et al. demonstrated the synthesis of AuNPs coated with alendronate which acts as a dual agent for chemotherapy and PTT in cancer treatment (Plan Sangnier et al. 2018). Alendronate is a nitrogen containing hydroxymethylene bisphosphonate, clinically available as adjuvant (Fosamax®) and can be efficiently utilized



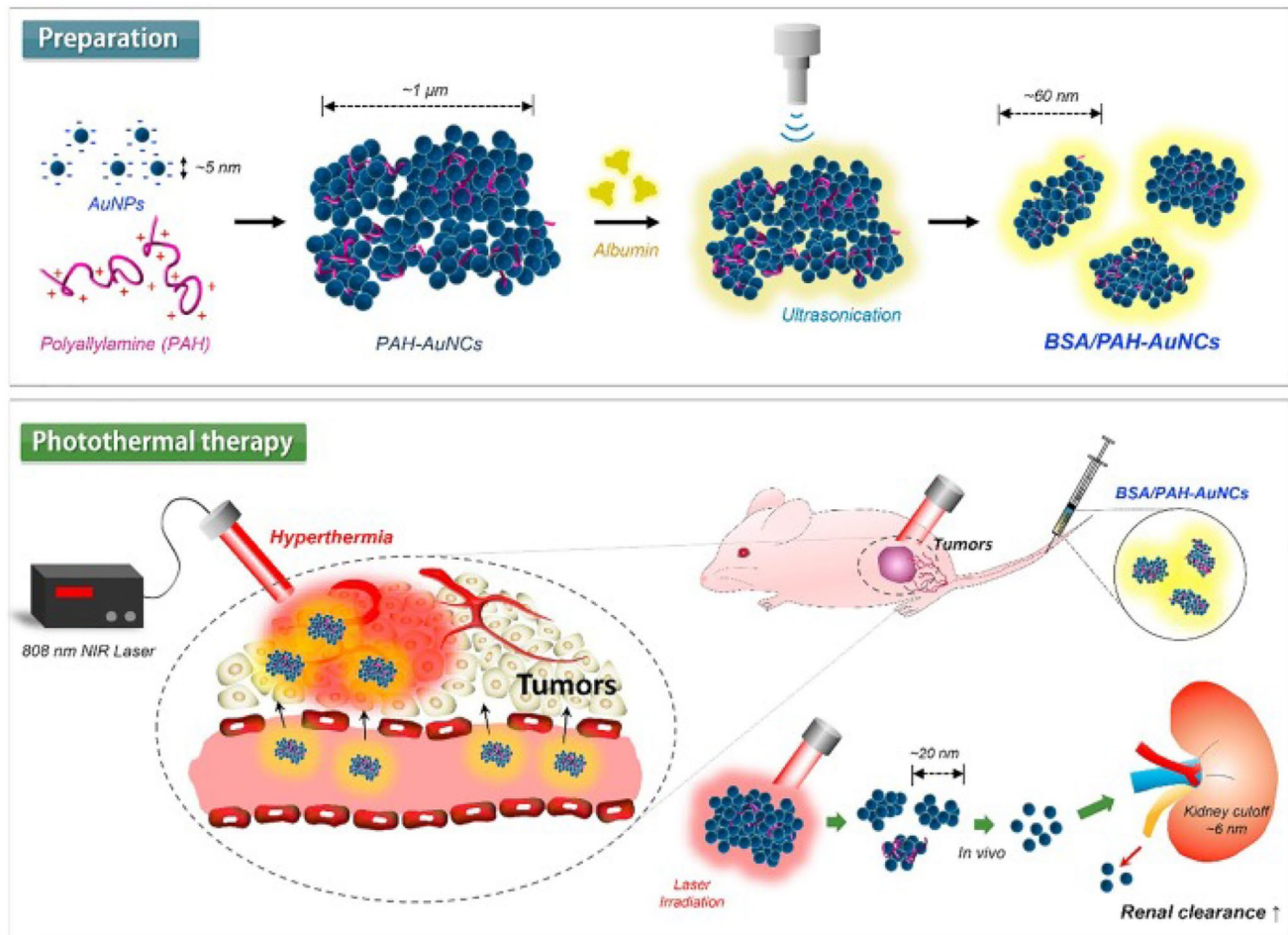


**Fig. 2** Schematic illustration of the facile preparation and photothermal antitumor therapy of BSA/PAH-AuNCs. Reprinted with permission from Lee et al. (2018), *International Journal of Pharmaceutics*. Copyright 2019, Elsevier (Lee et al. 2018)

in the treatment of prostate and metastatic cancers (Mundy 2002). Au@alendronate NPs can be applied for combined antitumor activity via drug delivery and PTT. Its exposure inhibits the proliferation of prostate cancer (PC3) cells, with IC<sub>50</sub> value of 100 μM, whereas, under NIR irradiation, temperature increase was observed and IC<sub>50</sub> value was reduced to 1 μM. Au@alendronate NPs can accumulate within the cells due to enhanced permeability retention (EPR) effect, as impaired lymphatic system within tumor cells cannot clear these NPs efficiently (Greish 2010).

Gold nanocages (AuNCs) are also widely used in cancer theranostic due to their biocompatibility, excellent stability and easy modification ability (Polasek et al. 2017). Other than these, AuNCs have several other unique properties like inner hollow space, capacity to transport various cargo and easy surface functionalization (Zhu et al. 2018; Pang et al. 2016). In comparison to single functionalized NPs, multifunctional NPs have been proved to be a better theranostic agent as it is capable of multimodal imaging diagnosis as well as targeted cancer therapy. In this context, Qui et al.

developed a nanosystem consisting hyaluronic acid (HA) modified AuNCs, functionalized with anti-Glypican-1 (anti-GPC1) antibody, oridonin (ORI), gadolinium (Gd) and Cy7 dye which enable its use in multimodal imaging [near-infrared fluorescence (NIRF) and magnetic resonance imaging (MRI)] (Qiu et al. 2018). In proposed nanosystem, GPC1 is used as theranostic target to enhance the accumulation of NPs at tumor sites as it is selectively overexpressed in pancreatic cancer cells (Herreros-Villanueva and Bujanda 2016). Conjugation of ORI with AuNCs efficiently increases its solubility, antitumor efficacy and cellular uptake in cancerous cells. Additionally, HA coating on AuNCs surface provides the binding sites for anti-GPC1 antibody, Cy7, Gd and also facilitate the pH and enzyme triggered delivery of ORI (Liu et al. 2018a). Result showed that this nanosystem significantly decreases the cell viability and increases the apoptosis in pancreatic cancer cells. In vivo study showed that ORI-GPC1-NPs also enable the multimodal imaging and targeted therapy in pancreatic tumor xenografted mice. ORI-GPC1-NPs are shown to be highly accumulated at tumor

site than ORI-NPs, which may be due to GPC-1-mediated active tumor targeting, and its fluorescence intensity remains high even after 48 h of injection. In vivo antitumor efficacy showed that ORI-GPC1-NPs have strong tumor inhibitory effect, as tumor weight was reduced in nanocomplex treated mice in comparison to saline treated mice. Thus, this multifunctional theranostic nanosystem is useful in early diagnosis and treatment of pancreatic cancer cells.

Ultrasmall AuNPs have core diameter of ~2–3 nm and have several advantageous features like long plasma half-life, enhanced tissue penetration and improved tumor accumulation (Zarschler et al. 2016; Liu et al. 2013). Ultrasmall AuNPs conjugated with potent maytansine analog DM1 (MTC-100038) are shown to be used in systemic drug delivery vehicle in hepatocellular carcinoma (HCC) treatment, as shown in Fig. 3 (Hale et al. 2019). DM1 is a microtubulin inhibitor and displays antitumor activity even in nanomolar range (Poon et al. 2013). However, it found a very narrow range of clinical utilization due to its poor tolerability and systemic side effects. To overcome its side effect and improved therapeutic index, DM1 can be conjugated to different platforms like antibody–drug conjugates to improved clinical oncotherapy effect (Diamantis and Banerji 2016). Conjugation of DM1 to AuNPs also improved its overall

tolerability and permit the administration of ~threefold higher drug in comparison of free drug. It displayed potent in vitro activity towards various hepatocellular primary cell lines and other cancerous cell lines. As shown in Fig. 3, in vivo tumor growth inhibition (TGI) value of MTC-100038 shows more tumor inhibition than sorafenib, and TGI value increases with increasing concentration of MTC-100038 and reaches up to 98.7% ( $p=0.01$ ) at a concentration of 450  $\mu\text{g}/\text{kg}$ . Further, luminescent measurement of this group after 38 days revealed slow tumor growth and reduced tumor mass than those of vehicle group. This data provides robust evidence towards use of MTC-100038 in treatment of HCC and also offers advantage over currently used standard drug, sorafenib. Hollow AuNPs (HAuNPs) are another candidate which serves as an excellent candidate for drug delivery purpose, as due to its cavity structure it provide high availability of internal and external surface and biocompatibility (Ren et al. 2015). Imanparast et al. demonstrated the synthesis of Mitoxantrone (MTX) encapsulated PEGylated HAuNPs and also studied their effect on different cancerous cell lines (Imanparast et al. 2018). MTX drug has been used in the treatment of several malignancies as it inhibits cancer cell proliferation by inhibiting topoisomerase II and disrupting DNA synthesis/repair (Khan et al. 2010). Combined effect

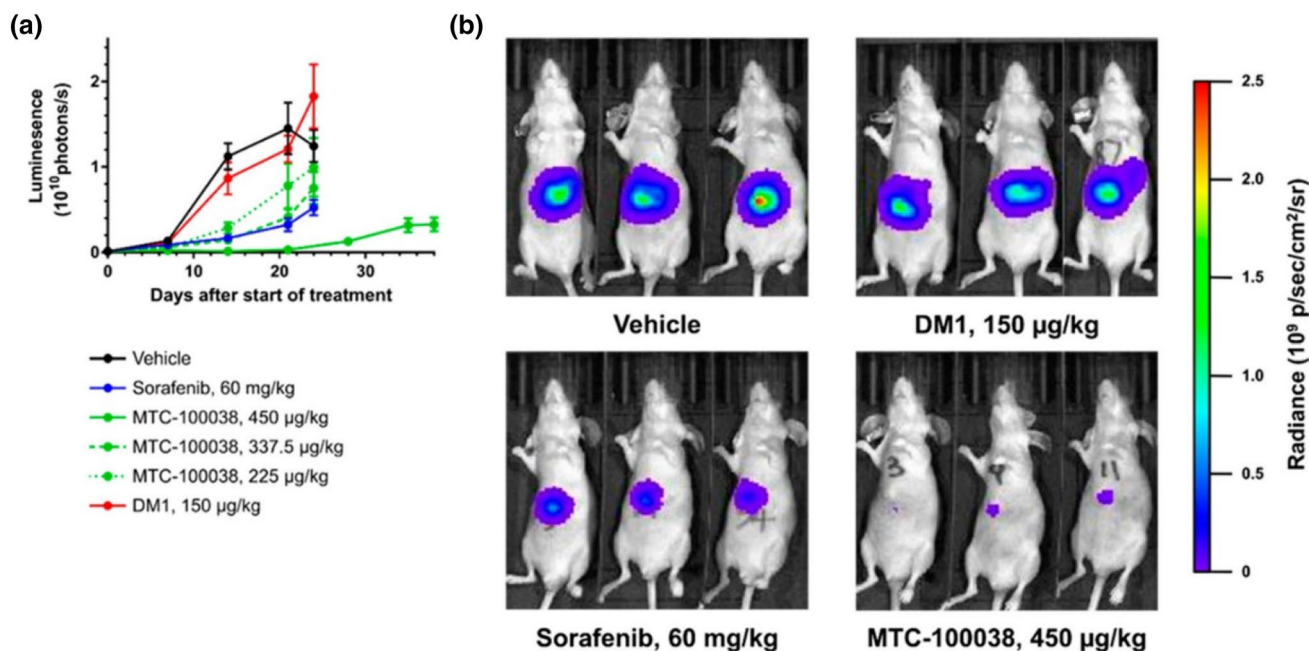


**Fig. 3** MTC-100038 treatment results in significant efficacy in orthotopic models of HCC and is better than the current standard of care sorafenib. Hep3B-Luc tumor cells were implanted into the left lobe of female BalbC/Nude mice. Mice ( $n=10/\text{group}$ ) received intravenous injection of either DM1, MTC-100038, or vehicle control for 2 dosing cycles of 5 consecutive days (QD5), separated by 5 days. The sorafenib treatment group received oral administration of 60 mg/kg daily for 21 days. Following administration of luciferin, tumor vol-

umes were visualized by measurement in a IVIS Lumina II imaging system: **a** tumor growth curves; **b** images of mice with tumors in situ showing significant differences in luminescence (tumor size) between treatment groups. MTC-100038 is an effect treatment agent. Error bars represent  $\pm$ SEM. Reprinted with permission from Hale et al. (2019), *Bioconjugate Chemistry*. Copyright 2019, American Chemical Society (Hale et al. 2019)

of PDT and chemotherapy of MTX conjugated HAuNPs has been studied. Result showed that MTX-AuNPs have improved efficacy of PDT with light emission diode (LED) and release of drug mainly depends on the radiant time and pH of the environment. Effect of PDT and chemotherapy was high in DFW cells than MCF-7 cells, may be due to the high resistant of breast cancer cells.

Among various reported NIR photothermal transducer, gold nanorods (AuNRs) possesses various advantages like enhanced biocompatibility and tunable SPR to convert NIR light into local heat and thus can be extensively utilized in biomedical purpose. Thus, AuNRs based PTT can be expected to work as an efficient anti-cancer agent alone or in combination with chemotherapeutic drugs (Hlapisi et al. 2019). In this context, Chen et al. demonstrated the synthesis of DOX conjugated pH-responsive AuNRs and also showed its application as a chemotherapeutic and PTT agent in treatment of liver cancer cells (Chen et al. 2018). DOX was conjugated to the AuNRs surface via pH-sensitive linkage (AuNRs@DOX) and ingested into HepG2 cells. It internalized into cells via endocytosis where the acidic pH triggers the release of DOX and leads to a chemotherapeutic effect. Apart from being drug carrier, AuNRs also acts as photothermal conversion agent and at 808 nm NIR laser, it significantly enhances the cytotoxicity and apoptosis in cancerous cells. Approximately 70–80% of triple-negative breast cancer (TNBC) cells express EGFR but lacks therapy strategies and only few EGFR targeting therapy produces positive results. AuNRs attached with anti-EGFR agent proved to be an excellent targeting agent in treatment of TNBC using photoacoustic imaging (PAI)-guided PTT (Zhang et al. 2017). Anti-EGFR agent in combination with PTT shows synergistic effect by anti-proliferative and apoptotic actions due to up regulation of HSP-70, and down-regulation of Ki-67 and EGFR proteins, and also inhibits intracellular signaling molecules in breast cancer cells.

Noninvasive transdermal drug delivery offers several advantages but it has been limited to few drugs which are small and lipophilic due to stratum corneum inevitable behavior. HA has now been considered as a promising transdermal delivery agent for NMs and proteins. HA penetration capacity enhances due to the presence of HA receptors on keratinocytes and fibroblasts in epidermis and dermis (Stellavato et al. 2016; Lee et al. 2016). Noninvasive transdermal delivery of HA and DR5 (death receptor 5 antibody) coated AuNRs provides a better platform for PA imaging mediated cancer therapy. DR5 Ab specifically targets the DR5 (belongs to tumor necrosis factor receptor family), which are overexpressed in cancer cell membrane, to induce apoptosis in cancer cells. HA coating on AuNRs surface enhances its stability and also prevents its non-specific interaction with serum protein in body. PA imaging and two-photon microscopy in in vivo study showed that complex can be delivered

transdermally via inevitable barrier of stratum corneum in skin and shows drastic reduction in tumor growth for up to 5 days. In cancer therapy, apoptosis is key process in elimination of cancer cells and releases cyto-c rapidly into cytoplasm and also in extracellular environment. Release of cyto-c from mitochondria into cytoplasm regarded as apoptosis point-of-no-return stage. Thus, cytochrome-c (cyto-c) is a key biomarker in detection of several diseases and also helps in determination of cancer therapy effect (Eleftheriadis et al. 2016). The concentration of cyto-c level in serum is directly proportional to the death of cancer cells i.e. effectiveness of anticancer drugs (Loo et al. 2017). A microfluidic platform was developed for sensitive detection of extracellular cyto-c using LSPR of aptamer conjugated AuNRs. Initially, cyto-c was adsorbed on the antibody functionalized micro-magnetic particles (MMP). Further, addition of aptamer conjugated AuNRs lead to the formation of sandwich-like structure with cyto-c i.e. (MMP-ab)-(cyto-c)-(AuNRs-aptamer). This sandwich complex leads to formation of AuNR aggregates which changes the LSPR signal in correspondence to amount of cyto-c. This platform exhibit detection limit of 0.1 ng/mL of cyto-c sparked in human serum and culture medium and requires 2 h for complete detection process. Thus, result confirmed that LSPR-AuNRs assay is an effective approach for determination of cyto-c concentration in serum.

In the detection of target analytes, colorimetric detection by artificial enzyme mimetic activity has been proved to be current research interest. Over natural enzyme, artificial enzyme offers several advantages like low-cost synthesis, high stability, and easy preparation steps. Au based nanomaterials like AuNPs and AuNCs are well reported for their catalytic peroxidase mimetic activity. 3,3',5,5'-tetramethylbenzidine (TMB) is chromogenic peroxidase substrate, which produces blue color upon oxidation with increasing absorbance at 652 nm. In this context, Feng et al. developed novel and facile method for colorimetric detection of cellular glutathione (GSH) based on its inhibiting effect on peroxidase-like activity of GSH stabilized AuNCs (Feng et al. 2017). GSH is the most abundant biothiol presents in cells which plays protective role in cells and also serves as key component in cellular metabolic functions. It is well reported that concentration of GSH level is much higher in cancerous cells than in normal cells which may offer opportunity to detect cancer cells at an early stage (Xianyu et al. 2015). In this proposed sensor, GSH inhibits the catalytic activity of AuNCs and thus also prevents the oxidation of peroxidase substrate, i.e. TMB to produce blue color. GSH acts as a reducing agent and scavenge  $\cdot\text{OH}$  radicals arises due to decomposition of  $\text{H}_2\text{O}_2$ , and thus suppresses the oxidation of TMB. The proposed sensing system can detect GSH concentration in linear range from 2 to 25  $\mu\text{M}$  with detection limit



of 420 nM. Graphene oxide (GO) conjugated AuNCs (GO-AuNCs) nanohybrid shows enhanced peroxidase-like activity with several advantages like low-cost synthesis, enhanced stability as well as catalytic activity over broad pH range including neutral pH (Tao et al. 2013). In contrast to AuNCs, GO-AuNCs shows 82% peroxidase activity at pH 7.0 compared to pH 3.0. Thus, FA conjugated GO-AuNCs nanohybrid can efficiently be utilized in cancer cell detection and novel substitute of peroxidase having high potential in bioanalytical chemistry. This method allows the detection of as low as 1000 MCF-7 cells. By using advantage of liposomes (LP) and artificial enzymes signal amplification technique, Tao et al. proposed AuNCs loaded liposomes conjugated with HER2 antibody for amplified colorimetric detection of HER2-positive breast cancer cells (Tao et al. 2017). It allows the identification of breast cancer cells with high sensitivity and selectivity. Cells conjugated with AuNCs-LP catalyzes the TMB oxidation in presence of PBST (PBS-Tween-20), where, tween-20 ruptures the liposome membrane to release AuNCs in surrounding environment. Oxidation of TMB can be easily monitored by recording the absorbance values. Result confirmed that the combination of enzymatic catalyzed reaction with liposome-enrichment resulted in improved detection of cancer cells, thus highlighting the potential of AuNCs as a promising diagnostic tool in oncology. Hu et al. proposed the FR targeting AuNCs as novel fluorescence as well as peroxidase enzyme mimetic nanoprobe (Hu et al. 2014). It can efficiently be utilized for tumor tissue fluorescence/visualizing detection. Complementary results were obtained when same tumor slices were detected by nanoprobe peroxidase staining (microscopic imaging with bright field) and fluorescence staining. Thus, fluorescence enzyme mimetic nanoprobe will provide molecular co-localization diagnosis technique which also helps to avoid false-negative and false-positive results. This aspect further improves the specificity and accuracy of cancer diagnosis. Analysis of various clinical samples demonstrates that nanoprobe can efficiently distinguish the cancerous cells from normal cells. In another approach, Maji et al. developed the hybrid nanocomplex consisting AuNPs and mesoporous silica-coated nanosized reduced GO conjugated with FA (GSF@AuNPs) and utilized it in peroxidase dependent detection of cancerous cells (Maji et al. 2015). This nanohybrid can be used as cancer therapeutic agent in presence of  $H_2O_2$  and ascorbic acid (AA). Result showed that in HeLa cells, cytotoxicity of nanohybrid is due to the formation of reactive oxygen species (ROS) in presence of GSF@AuNPs together with endogenous or exogenous  $H_2O_2$  and AA. This nanohybrid was also tested for toxicity in normal HEK 293 cells and result showed that it does not induce damage to normal cells in the presence of  $H_2O_2$  and AA, thus proving the

selective killing activity of cancerous cells by GSF@AuNPs nanohybrid. Table 2 summarizes the more application of AuNPs in diagnostic and treatment of cancer cells.

## Iron oxide nanoparticles

Iron oxide NPs (IONPs) have found several applications in biomedicine field and most widely used as a contrast probe in MRI. In strong magnetic field, IONPs create microscopic field gradient which causes shortening or diphasic of longitudinal (T1) or transverse relaxation times (T2) of nuclei around, mostly protons. It further induces hypo- (for T2) and hyper- intensities (for T1) on MRI map thus highlighting the particles accumulated area. IONPs can be efficiently used in lymph node imaging, liver imaging and cell tracking applications (Chen et al. 2013). Tseng et al. developed a superparamagnetic iron oxide NPs (SPIONs) based theranostic platform where dextran-coated SPIONs were conjugated with anti- EGFR monoclonal antibody and cetuximab (cet-PEG-dexSPIONs) via periodate oxidation (Tseng et al. 2015). Modification of dextran-coated magnetic nanoprobe with dihydrazide-PEG reduces the non-specific binding under biological conditions. Preclinical studies validated the antitumor activity of cetuximab, it acts by G0/G1 cell cycle arrest, apoptosis induction, DNA repair alteration, metastasis, and angiogenesis inhibition (Tseng et al. 2015; Park et al. 2016). Cetuximab modified NPs acts as a targeting moiety to recognize EGFR overexpressing cancerous cells and thus can be used for therapeutic and diagnostic purposes. EGFR has been documented to be overexpressed in nearly one-third of epithelial malignancies (Ho et al. 2012) and thus can be diagnosed with as proposed nanosystem. Result showed that cet-PEG-dexSPIONs binds specifically to EGFR overexpressing cancerous cells and thus can enhance the image contrast on MRI. Exposure of cet-PEG-dexSPIONs showed significant increase in apoptotic population of A431 cells in comparison to cetuximab alone. These therapeutic effects may be due to the multivalency of resulting magnetic nanoprobe. Cet-PEG-dexSPIONs also showed to exhibit antibody-dependent cellular cytotoxicity (ADCC) effect with ~ 10.4% target cell lysis. In addition to inhibit the EGF induced EGFR phosphorylation this nanosystem also enhanced internalization and degradation of EGFR. In vitro studies demonstrate the receptor-mediated endocytosis of cet-PEG-dexSPIONs which enables ultrasensitive tumor imaging and thus proved to be an excellent contrast agent in MRI. Various chemotherapeutics are systemically administered into body but only small amount of dose reaches to tumor site. Thus, there is an urgent requirement to find way by which drugs mainly accumulate at targeted sites and its concentration remains decreased in rest of the

**Table 2** Application of gold nanomaterials in cancer detection and therapy

Nanosystem	Target molecule/drug	Cell line/animals	Application	Result	References
Au@Ag core-shell nanoprobe	FA	MGC-803 cells	Surface-enhanced Raman scattering (SERS) activity	Nanoprobes exhibit excellent detection ability of living cancer cells	Chang et al. (2019b)
Gold nanostar	Matrix metalloproteinase 2, IR-780 iodide	A549 cells	NIR imaging, PA imaging, PDT	Suppressed the growth of tumor, and the tumor volume decreased by 93%	Xia et al. (2019)
AuNPs	Chlorotoxin (CTX), radioc chloride <sup>131</sup> I	BALB/c female nude mice	SPECT/computed tomography (CT) imaging, radionuclide therapy	Due to CTX, the developed nanoprobe can cross the Blood-Brain Barrier (BBB) and specifically target glioma cells in a rat intracranial glioma model	Zhao et al. (2019b)
Au@Cu3 1,3,5-benzenetricarboxylate NPs	Aptamer, DOX	A549, BEAS-2B and HeLa cells	SERS imaging, chemo, and PT therapy	Nanosystem exhibited high drug loading capacity (57%). Effective in cell tracking and in vivo synergistic therapy	He et al. (2019)
Magnetic AuNPs	DOX	MCF7 cells and Female Swiss mice	Contrast agent for MRI, chemo and PT therapy	Iron core allows the magnetic targeting of particles to tumor sites. Nanocomposite have the ability to visualize and kill tumor cells with high precision	Elbially et al. (2019)
AuNPs	PPP-CD-g-PEG	U87 and Vero cells	Fluorescence cell imaging and radiotherapy	Radiosensitivity efficiently increases with the use of this conjugate	Barlas et al. (2019)
AuNPs/Gold sulphide (AuS) NPs	C225 (Cetuximab monoclonal antibody)	MDA MB 231 and A549 cells	PTT	PTT can reduce the cell survival to less than 20%	Ramezanzadeh et al. (2018)
AuNPs	–	HSC-3 cells	–	Combination of 4 Gy irradiation with AuNPs significantly increases the apoptotic cells	Teraoka et al. (2018)

PPP-CD-g-PEG poly(*p*-phenylene-co-cyclodextrin-*g*-poly(ethylene glycol))

body. Magnetic drug targeting (MDT) can be utilized for targeted drug delivery where drug loaded magnetic nanoparticles are injected into the vascular system upstream from the malignant tissue and captured at the tumor site using an applied magnetic field (Lyer et al. 2015). In similar context, Lugert et al. have developed lauric acid (LA) and human serum albumin (HSA) coated SPIONs and utilized it as paclitaxel (Ptx) carrier (LA-HSA-Ptx SPIONs) for MDT purpose (Lugert et al. 2019). Authors have investigated the effect of LA-HSA-Ptx SPIONs in 2D and 3D cell cultures. Result showed that binding of antiproliferative and antitumorigenic agent, paclitaxel to SPIONs shows significant effect in different breast cancer cell lines without affecting the cytotoxic efficiency of chemotherapeutic drug. Authors have also assessed the apoptotic effect, membrane damaging potential and cell cycle effect of Ptx and Ptx bound particles in a concentration-, time- and cell-dependent manner. Interestingly, Ptx and LA-HSA-Ptx SPIONs showed similar toxic effect which dismissed the chance of structural alteration or masking effect. In 3D culture model, progression of MDA-MB-231 and T-47D spheroids were completely inhibited after 24 h in presence of free and SPIONs bound Ptx followed by constant shrinking, whereas, BT-474 cells displayed complete inhibition after 5 days. Although MRI has an excellent spatial resolution, but its application in cancer diagnosis is limited due to its poor sensitivity (Liu et al. 2016a). In contrast to this, NIRF imaging exhibits high sensitivity but has poor resolution and limited penetration depth (Key et al. 2012). Indocyanine green (ICG) dye exhibits maximal absorption and emission in NIR region and also only FDA approved NIR organic dye. It has also been reported earlier that SPIONs loaded with ICG can effectively enhance the photoacoustic tomography of brain vasculature and tumor (Gao et al. 2016). Thus, for dual function of targeted drug delivery to tumor sites as well as contrast images acquisition, an optimal multifunctional NPs which consist of bimodal imaging and chemotherapy effect will be required. In this context, Shen et al. constructed multifunctional drug delivery system capable of real time MRI, chemotherapeutic effect as well as fluorescence imaging in orthotopic glioma model (Shen et al. 2019). It consists of SPIONs coated with 1,2-distearoyl-sn-glycero-3-phosphoethanolamine-*N*-[methoxy (polyethylene glycol)-2000] (DSPE-PEG-2000) which further conjugated with DOX and ICG into lipid shell layer across NPs surface (SPIO@DSPE-PEG/DOX/ICG NPs). SPIONs here serve for real time MRI whereas, lipid shell around SPIONs acts as carrier for DOX and ICG (real time fluorescence imaging). Result showed that SPIO@DSPE-PEG/DOX/ICG NPs exhibits significant DOX internalization in comparison to free drug. It also crosses the blood brain barrier (BBB) and selectively accumulates at the tumor

site. Among all groups, NPs treated C6 glioma bearing rat exhibit maximum therapeutic effect which includes less body weight loss, longest survival time, small tumor volume with no obvious side effects.

Aptamers are single-stranded RNA or DNA oligonucleotides and can be folded into 3D conformations with high binding affinity and specificity. Aptamers are relatively small in size which allows their efficient penetration into tumor and also enhances its retention time (Xiang et al. 2015). Aptamers due to these properties are proved to be an ideal option for preparing multifunctional target specific NPs (Zhang et al. 2018; Xiao et al. 2012). Zhao et al. also demonstrated the synthesis of aptamer functionalized IONPs@carbon@DOX NPs (Apt-Fe<sub>3</sub>O<sub>4</sub>@C@DOX) and also showed its synergistic chemo-PTT effect in cancer therapy both in vitro and in vivo (Fig. 4) (Zhao et al. 2019a). Result showed that Apt-Fe<sub>3</sub>O<sub>4</sub>@C@DOX exhibit high capacity to translate incident 808 nm NIR light into heat energy and extensive pH/heat-induced drug release ability. In vitro studies showed that combined chemo-PTT therapy is more toxic than PTT or chemotherapy alone in A549 cells. It has exceptional tumor targeting ability and thus allowed simultaneous tumor detection via MRI. This therapy significantly decreases the tumor growth rate even at small DOX concentration due to photothermal effect induced intracellular heat generation, which can reduce the DOX metabolism and thus leads to increase in drug concentration in cancerous cells. As shown in Fig. 4, laser irradiation improves the therapeutic effect of nanocomplex due to its increased tumor uptake by EPR effect and aptamer targeting. Treatment of Apt-Fe<sub>3</sub>O<sub>4</sub>@C with NIR leads to partial delay in tumor growth whereas, Apt-Fe<sub>3</sub>O<sub>4</sub>@C@DOX exposure with NIR demonstrated the complete eradication of tumor. This data was also strongly supported by the hematoxylin and eosin (H&E) staining of tumor, as in control group, tumor retained its normal morphology with distinctive nuclear structure and membrane whereas, in combination therapy group, tumor can be barely observed. In another report, Kale et al. demonstrated the synthesis of iron oxide-gadolinium-containing Prussian blue NPs (IONPs@GdPB) and their application as a theranostic agent for T1-weighted MRI and PTT in tumor (Kale et al. 2017). Result clearly showed that NPs retained their photothermal heating property for four cycles of heating and cooling which indicate their stability as photothermal activity over multiple heating cycles and its photothermal conversion efficiency was found to be 16.1%. In the absence of NIR radiation, IONPs@GdPB shows only marginal intrinsic toxicity, whereas, upon NIR irradiation, significant increase in toxicity was observed which corresponds to decrease in cell viability (<60%). Ex vivo imaging result displayed that NPs shows increased signal:noise ratio in T1 W scans of tumor phantoms in comparison to control. Thus, synthesized nanocomplex function as an efficient PTT agent in vivo with

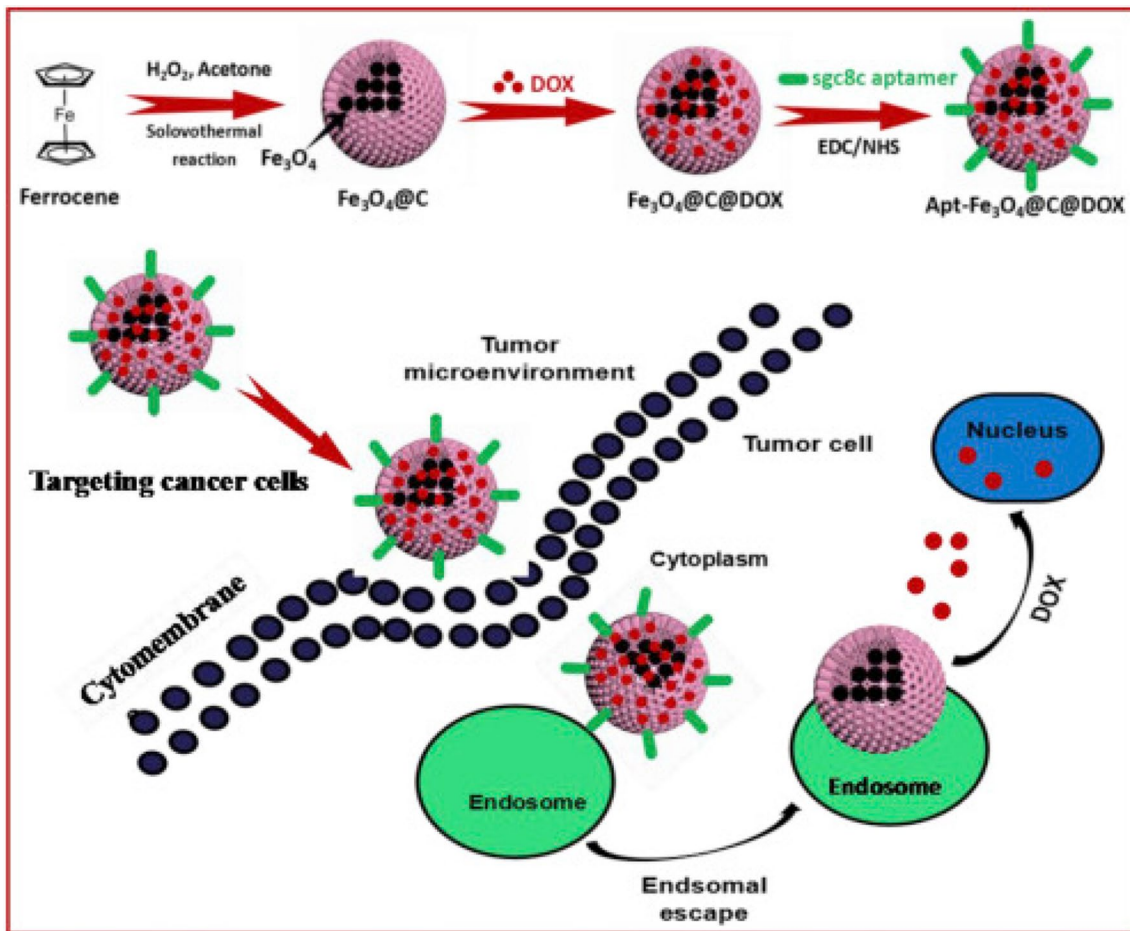


**Fig. 4** Schematic of the preparation of Apt-IONPs@C@doxorubicin (DOX) NPs and internalization of Apt-IONPs@C@DOX NPs into cancer cells for chemo–photothermal combination therapy. Reprinted

with permission from Zhao et al. (2019a), *Analytica Chimica Acta*. Copyright 2019, Elsevier (Zhao et al. 2019a)

decreased tumor growth rate and increased survival rate in comparison of untreated control. Table 3 summarizes the more application of IONPs in diagnosis and treatment of cancer cells.

IONPs have been reported to exhibit intrinsic peroxidase-like activity and it depends on the particle's structure and morphology. Fu et al. prepared the different structured of IONPs i.e. nanoclusters, nanoflowers and nanodiamonds by tuning pH value in hydrothermal reaction. Result showed that nanostructures have great influence on peroxidase activity assay in the order, nanoclusters > nanoflowers > nanodiamonds (Fu et al. 2017). Nanoclusters have high enzymatic activity due to its large surface area, porous structure, and smallest crystalline size than nanoflowers and nanodiamonds. By utilizing the peroxidase activity, authors have used it in cancer therapy application at ultralow concentration of  $H_2O_2$ . Cytotoxic activity of IONPs is reported to be due to the generation of intracellular ROS upon endocytosis into cancerous cells. However, anti-cancer effect of

IONPs was not consistent with their in vitro peroxidase-like activity. Thus, it can be concluded that, in addition to enzyme-like activity, cellular internalization of particles also contributed to the cancer cell killing effect. In addition to structure, chemical composition, shape and size of particles also have great influence on catalytic activity of IONPs (Peng et al. 2015). Four different sizes (4, 16, 18 and 27 nm) and shape of MnIONPs were investigated for their catalytic peroxide reaction in aqueous media. Peroxidase activity of these NPs are found to be shape- and size-dependent in order of 4 nm (spherical) > 18 nm (plate-like) > 27 nm (near-cubic) > 16 nm (spherical) (Fig. 5). Proposed order is closely related to the surface-to-volume ratio and atom arrangements. For particle of similar shape, catalytic activity increases with decreasing particle size which may be due to the high surface area to volume ratio of smaller particles. However, with the increase in particle size their catalytic activity depends on shape also, due to the fact that different crystal plane exhibit different atomic arrangement which



**Table 3** Various applications of iron oxide nanoparticles in cancer detection and therapy

Nanosystem	Target molecule/drug	Cell line/animals	Application	Result	References
IONPs	FA	KB cells and Nude BALB/c female mice	MRI	It shows great potential as a contrast agent in MRI, as well as in the combination with drug delivery for cancer therapy	Vu-Quang et al. (2019)
IONPs	DOX		In vivo imaging and anti-tumor activity experiments	Realize the diagnosis and treatment of malignant tumor at the same time	Jie et al. (2019)
IONPs	10-hydroxy camptothecin, HCPT	MCF-7, 3T3, 4T1 cell lines and BALB/c mice	Contrast agent for MR imaging, PTT and chemotherapy	IONPs elicits the generation of ROS with the presence of macrophage, which can further inhibit the growth of cancer cell	Li et al. (2019b)
IONPs	DOX	–	MR contrast agent	Theragnostic application due to low toxicity, MRI character, passive and magnetic targeting properties.	Kim et al. (2018)
Egg albumin coated IONPs	5- Fluorouracil	L-929 fibroblast cells	Swelling control and magnetic field mediated drug delivery	Release behavior of drug depends on swelling ratio, pH, temperature and simulated fluids	Sonker et al. (2018)
IO/carbon NPs	hydroxypropyl- $\beta$ -cyclodextrin, DOX	4T1 cells	MR/NIRFL dual-modal imaging	NIR induced heat also increases the drug permeation. Tumor inhibition was recorded due to synergistic chemo/PT therapy	Song et al. (2018)
Cobalt IONPs	FA, DOX	Peripheral blood mononuclear cells (PBMC)	Magnetic field- induced hyperthermia	Drug release increases at higher temperature and acidic pH. Synthesized nanoconjugate was biocompatible in nature	Dey et al. (2018)

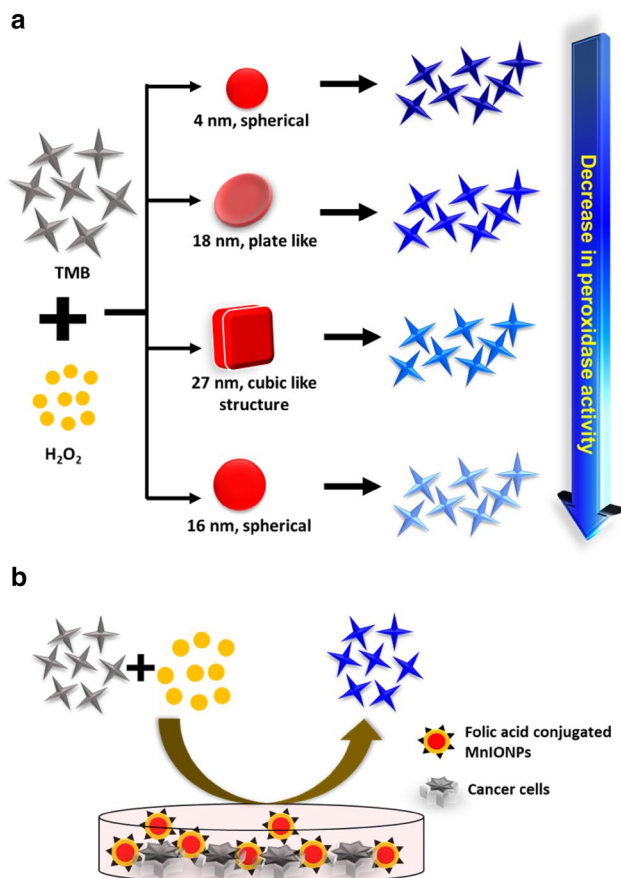


**Fig. 5** **a** Schematic showing shape and size-dependent peroxidase mimetic activity of MnIONPs. **b** FA conjugated MnIONPs in FR expressing cancer cell diagnosis by utilizing its enzymatic activity

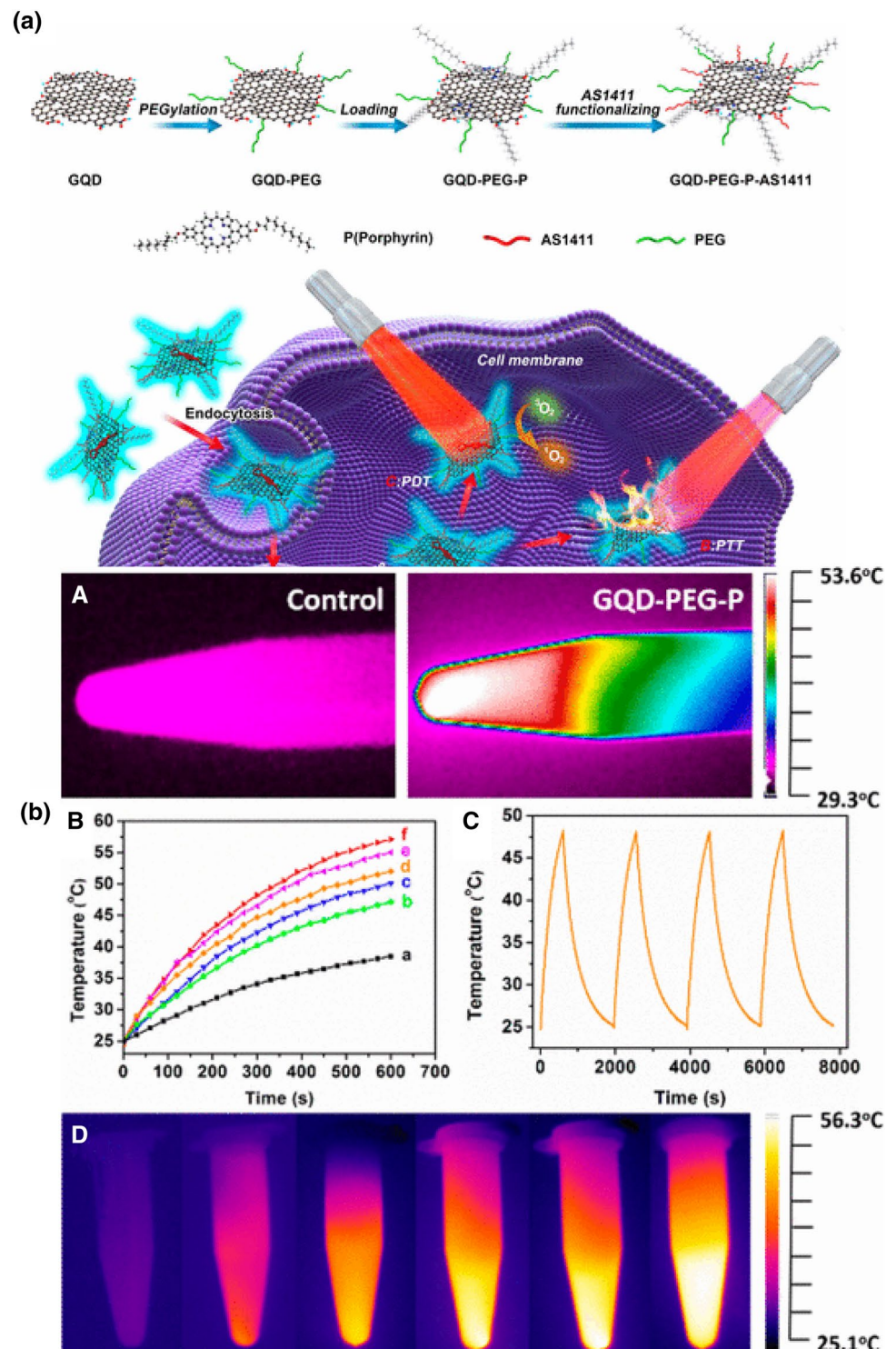
governs the reactivity and selectivity of particles. NPs were further conjugated with FA and fluorescein isothiocyanate (FITC) to target cancerous cells and verified if it can replace horseradish peroxidase (HRP) in an immunoassay. Result showed that it can clearly discriminate the FR positive cancerous cells from FR negative normal cells, with detection limit of 100 cells. It further utilized in fluorescent visualization of target cells also, due to its peroxidase mediated tyramide signal amplification which generates high fluorescence in target biomolecules in situ. In a similar way to HRP, MnIONPs also binds to FITC and shows site-specific enhanced fluorescence signal. Fluorescence signal in FR positive cancerous cells was high due to the strong FA affinity in comparison to FR negative normal cells.

## Quantum dots

Quantum dots (QDs) have several unique properties like high drug loading capacity, biocompatibility, strong photoluminescence, excellent physiological stability and facile

production which enable its wide application in biomedical purpose (Chen et al. 2017b). Cao et al. synthesized the multifunctional theranostic platform by conjugating porphyrin derivative with PEGylated and aptamer functionalized graphene quantum dots (GQDs) with an excellent fluorescent property (GQDs-PEG-P) (Fig. 6a) (Cao et al. 2017). Porphyrin and its derivatives are known to exhibit singlet oxygen generating ability and low toxicity which make them suitable candidate to be used as second generation photosensitizers (Kou et al. 2017). In PDT process, photosensitizer molecules transfer the photon energy to surrounding oxygen molecule which generates ROS like singlet oxygen for elimination of cancerous cells when irradiated with light of appropriate wavelength (Cheng et al. 2015; Tian et al. 2013). However, its low cellular uptake efficiency, hydrophobicity, and poor physiological stability limit its application in biomedicine (Chung et al. 2016; Liu et al. 2016b). To overcome this problem, porphyrin can be conjugated to GQDs which exhibit exceptional biocompatibility, low toxicity, and excellent physiological stability. Thus, comprised nanosystem shows dual ability of porphyrin induced high singlet oxygen generation and GQDs based excellent optical properties. By utilizing the comprised nanosystem, cancer cells can be discriminated from somatic cells due to intrinsic fluorescence property of GQDs, whereas, its high surface area facilitates the gene delivery for detection of cancer related microRNA (miRNA). Result showed that constructed nanosystem displayed photothermal conversion efficiency of 28.58% and high quantum yield of singlet oxygen generation (1.08) which enabled its application in PTT and PDT for cancer treatment. As shown in Fig. 6b, upon irradiation with 980 nm laser for 10 min, temperature of GQDs-PEG-P rises to 53.6 °C whereas, in case of water it is only 33.2 °C. This system also shows good reproducibility and excellent stability after each on/off cycle of laser light. When tested with A549 cells, system temperature reached to photoablation limit of 46 °C within 5 min of radiation exposure and 56.3 °C after 10 min. This high temperature produces enormous heat in cancer cells for cancer ablation. Also, cell membrane destruction and early apoptosis were observed in GQDs-PEG-P treated A549 cells even at low laser power. Thus combined synergistic PTT and PDT effect led to excellent therapeutic efficiency in cancer therapy (Cao et al. 2017). Mutation is considered as one of the major cause for induction of cancer. DNA lesion 8-oxoguanine (8-oxoG) is most common oxidative damage which leads to G:C to T:A transversions and thus induces cancer in humans (Viel et al. 2017). Human 8-oxoG DNA glycosylase I (hOGG1) is a key enzyme involved in 8-oxoG base removal thus its level is related to different types of cancer (Hu et al. 2018). In this context, Jie et al. demonstrated the novel multifunctional DNA nanocage

**Fig. 6 a** Synthesis of GQD-PEG-P and Schematic Presentation of GO-PEG-P Theranostic Platform for Intracellular miRNA Detection and the Combined Photothermal/Photodynamic Therapy. **b** Photothermal profile of GQD-PEG-P. **a** Thermal images of vials containing water and GQD-PEG-P solution (100  $\mu\text{g}/\text{mL}$ ). **b** Photothermal heating curves of water (**a**) and (**b–f**) solutions containing GQD-PEG-P at different concentration (10, 25, 50, 100, and 200  $\mu\text{g}/\text{mL}$ ); **c** photothermal effect of the NIR irradiation to GQD-PEG-P solutions (100  $\mu\text{g}/\text{mL}$ ) with the NIR laser was shut off after irradiation for 10 min. **d** Thermal images taken with 2 min interval of vials containing pellets of GQD-PEG-P-exposed A549 cells at the concentration of 100  $\mu\text{g}/\text{mL}$ . Reprinted with permission from Cao et al. (2017), *Applied Materials*. Copyright 2017, American Chemical Society (Cao et al. 2017)



labeled with cadmium tellurium (CdTe) QDs signal probe (Jie et al. 2019). It can be utilized for sensitive fluorometric detection of hOGG1 by exonuclease (Exo III)-assisted cycling amplification strategy and also loaded with DOX to serve both as fluorescence imaging and chemotherapeutic agent (Fig. 7). Firstly, DNA template containing

8-oxoG (DNA HP1) was designed, which can be selectively cleaved by hOGG1 enzyme, to form new DNA fragment (DNA2). Further, DNA HP2 was added into system which hybridized with DNA2 to form new duplex DNA with recessed 3-terminus which again digested with ExoIII and cycling amplification process was initiated (cycle I)



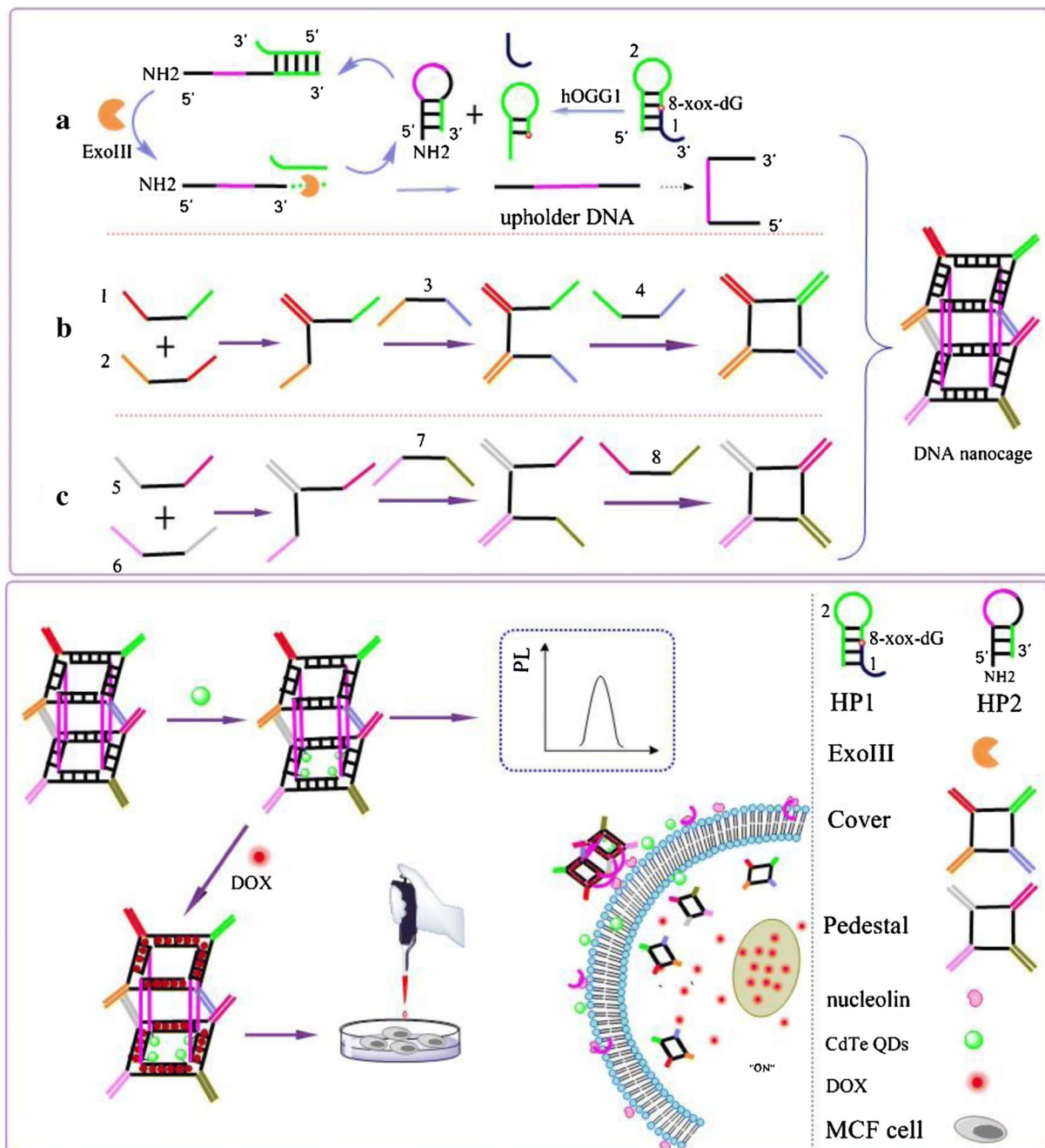


**Fig. 7** A multifunctional DNA nanocage containing CdTe quantum dots and acting as a signalling probe was prepared. It was applied to fluorometric determination of human 8-oxoG DNA glycosylase 1 using cycling amplification technique. It also enables drug delivery

to cancer cells if loaded with doxorubicin. Reprinted with permission from Jie et al. (2019), *Microchimica Acta*. Copyright 2019, Springer Nature (Jie et al. 2019)

which releases enormous amount of HP2 DNA fragment (unholder DNA). This unholder DNA contains nucleolin aptamer (violet) and fragment linking Cover and Pedestal DNA (black). Finally, hexahedral DNA nanocage was formed by combination of unholder DNA, cover DNA and Pedestal DNA, which was further conjugated with fluorescent CdTe QDs for sensitive detection of hoGG1. Finally,

DOX recognizes the G:C bases and embedded into DNA nanocage which turns OFF the fluorescence of DOX. Studies showed that fluorescence of DOX can be reduced by double chain structure (Chan et al. 2016) and presence of QDs also inhibit its fluorescence, thus formation of DNA nanocage can be preliminary determined by fluorescence of DOX. DNA nanocage targets and enters the cancerous



MCF-7 cells by specific binding of aptamer to nucleolin of cells. Further DNA nanocage disperses and DOX was released into cells which can turn “ON” the fluorescence of DOX. This, proposed nanosystem offers both fluorescence imaging and targeted drug delivery to cancer cells and also shows good analytical performance for hOGG1 detection in diluted cell lysates to display great potential for real biological experiments. Prostate stem cell antigen (PSCA) is prostate tumor-associated antigen and reported to be overexpressed in prostate, kidney, and bladder cancer (Liu et al. 2017). For PSCA mediated diagnosis of bladder urothelial cancer, Yuan et al. synthesized the QDs605 conjugated with PSCA monoclonal antibody (QD-PSCA) by covalent coupling (Yuan et al. 2018) and utilized it for specific fluorescence imaging in EJ human bladder urothelial cancer cell line. Result showed that, over time, QD-PSCA appeared in cytoplasm which indicates cellular proliferation and endocytosis. Due to cell division and culture medium, average fluorescence intensity can be diminished gradually but remain visible even after 48 h of exposure. Thus, fluorescence intensity of QD-PSCA probe is highly stable which enable its use in early diagnosis, targeted therapy and imaging localization of tumor. Maximum studies shows the cancer therapy by utilizing chemotherapeutic drugs, however, Bansal et al. (Bansal et al. 2019) demonstrated the use of biosurfactant which proved to have minimum side effect, less toxicity and more biodegradability. Authors have analyzed the properties of biosurfactant (isolated from *Candida parapsilosis*) by using GQDs as nanocarrier. Biosurfactant conjugation to GQDs significantly reduces the cell viability in time- and dose-dependent manner. Viability of cells remains to be 90% when exposed to GQDs alone at concentration of 1 mg/ml, however in presence of biosurfactant 50% reduction in cell viability was observed within 24 h. Folate conjugation of GQDs nanoprobe enhanced its uptake in cancerous cells by receptor-mediated endocytosis in comparison to GQDs alone. In another study, Nasrollahi et al. conjugated the GQDs with antibody single-chain variable fragment (scFv), which has high affinity (GQDs-scFvB10) for EGFR (Nasrollahi et al. 2019). Surface of targeted GQDs exhibit high cisplatin (CsPt) loading capacity (50%) and also pH dependent release with slow release rate in neutral condition to reduce the systemic cytotoxic effect. Drug release kinetics showed that after 6 h, ~55% of drug was released at acidic pH of 5.5 whereas only 20% of drug was released at neutral pH of 7.4, within same time period. Higher release in acidic condition can be attributed due to protonation of GQDs functional group and neutralization of negative charge. CsPt loaded targeted GQDs nanocarrier demonstrated the significantly higher toxicity to MDA MD 231 cells in comparison to non-targeted drug due to its maximum uptake via EGFR. Lower uptake

and cytotoxicity was seen in cells having saturated EGFR which further demonstrate the selectivity of nanocarrier towards EGFR overexpressing cells.

Carbon dots (CDs) have also found its role in biomedical application due to its multiple surface chemical properties and thus can be conjugated with chemotherapeutic drugs (Feng et al. 2016), photothermal agents (Pandey et al. 2013), DNA/RNA (Pierrat et al. 2015) and photosensitizers (Huang et al. 2012) for efficient therapy and real-time monitoring. Various reports suggest that CDs have some intrinsic theranostic properties to kill tumor cells (Sun et al. 2016; Ge et al. 2015). Luo et al. have demonstrated that engineered fluorescent CDs can efficiently utilized in the cancer immunotherapy (Luo et al. 2018). Authors have synthesized nanocomposites consist of uniform-sized CDs and tumor model antigen protein ovalbumin (OVA), which can stimulate the dendritic cell maturation and corresponding T cell proliferation. Dendritic cells are important in cancer immunotherapy as it plays crucial role in specialize recognition and processing of antigens (Gardner and Ruffell 2016). Further, activated dendritic cells migrate to lymph nodes and present combination of antigen peptide with major histocompatibility complex (MHC) to activate T-cells which can target tumor cells expressing this antigen and then induces effective cytotoxic T-cells (CTL) response (Turnis and Rooney 2010). Result showed that proposed nanocomposites can suppress the B-16-OVA melanoma tumor growth. This nanoplatform thus can be employed to avoid degradation of tumor antigen proteins in complex physiological environments. Abdelahmid et al. synthesized tumor targeted QDs based theranostic nanocapsules (NCAPs) loaded with honokiol (HNK) and celecoxib (CXB) for breast cancer therapy (Abdelahmid et al. 2018). In order to overcome the poor water solubility, these two drugs were dissolved in the oil reservoir. Further, layer of anionic polysaccharide, chondroitin sulfate (CS) and lactoferrin (LF) were layer-by-layer assembled over the QDs to enhance its targeting and cellular internalization via CD44-mediated endocytosis (Lo et al. 2015). LF has its effect on apoptosis and proliferation of cancer cells and its biological properties depend on specific receptors present on cancer cell surface (Pandey et al. 2015; Mehra et al. 2013). Due to electron/energy transfer mechanism, luminescence of QDs was switched off upon conjugation with LF. Whereas, luminescence can be restored upon intracellular uptake of nanoprobe which enable its tracing for diagnosis purposes (Mitra et al. 2012). In assembly with NCAPs, HNK and CXB shows very slow release rate in comparison of free drugs. It was also seen that release rate of HNK is lower than that of CXB due to its higher log *p* value. LF coating over NCs significantly enhanced its cytotoxicity may be due to adsorptive mediated transcytosis mechanism of LC. Additionally, coupling of QDs with NCs lowers the IC<sub>50</sub> value by 1.21 and 1.13 fold (in comparison

of LF-CS-NCs) after 48 h exposure to MCF-7 and MDA MB-231 cells, respectively. In vivo study also showed that mice treated with LF-QDs-CS-NCs exhibit reduced tumor growth in comparison to other treated groups. Histopathological analysis showed that LF-QDs-CS-NCs treated mice have higher necrosis effect than control group. Moreover, treatment of LF-QDs-CS-NCs also reduces the expression of Ki-67 thus confirming its potential effect to inhibit cell proliferation by suppressing the tumor growth. Thus, antitumor effect of nanocarrier was displayed by enhanced cytotoxicity, reduced tumor volume and also by reduced p-AKT level, activation of apoptotic enzyme, caspase-3 and also inhibit angiogenic tumor marker VEGF-1. Thus, as prepared multifunctional nanoplateform acts as potential theranostic agent for imaging and targeted therapy. Table 4 summarizes the more research work related to application of QDs in therapy and diagnosis of cancer cells.

### Upconversion nanoparticles

Lanthanide based upconversion nanoparticles (UCNPs) have found their application in biomedical purpose as they can act as delivery agent of photosensitizer and also able to convert NIR light to ultraviolet/visible light via multiple-photon absorption which further helps to activate the photosensitizer in deep inside tissue (Wang et al. 2013a; Dong et al. 2015). In comparison of traditionally used organic fluorophores, UCNPs exhibit several advantages like long fluorescence time, very less autofluorescence background, induces less photodamage as well as deep tissue penetration (Chen et al. 2014; Fukaminato et al. 2018). In this context, Gracia et al. (Ramirez-Garcia et al. 2018) reported a novel NaYF<sub>4</sub>:Yb,Er-ZnPc-Trastuzumab theranostic nanoconjugate for tracking and PDT of HER2 positive cells (Fig. 8). Upon 975 nm NIR exposure NaYF<sub>4</sub>:Yb acts as nanotransducer and helps in conversion of deep penetrating NIR photons to red light which can be further used in cell tracking, optical imaging and activation of covalently attached zinc tetra substituted carboxyphenoxy phthalocyanine (ZnPc) by resonant energy transfer. Free ZnPc in water shows excitation spectra at 675 nm, and emission spectra of UCNPs was recorded at 659 nm corresponds to overlap of upconversion emission with ZnPc absorption peak. Further, activation of ZnPc leads to generation of singlet oxygen molecules by absorbing the red energy emitted from UCNPs by Förster Resonance Energy Transfer (FRET) process. In the absence of light this nanoconjugate is shown to be inert but shows significant reduction in HER2 expressing cell viability (up to 21%) upon short term irradiation of 5 min. Upon exposure of 975 nm light, singlet oxygen production was demonstrated by nanoconjugates and can be used for PDT purpose. Mancic et al. demonstrated the novel hybrid NaYF<sub>4</sub>:Yb,Er/

poly(lactic-co-glycolic acid) (PLGA) NPs for NIR excited fluorescence imaging of human mucosal cells (Mancic et al. 2018). Due to upconversion, both green and red emission are prominent in spectra but finally yields output of green light. Here, PLGA group provides excellent biocompatibility to nanoconjugates without compromising upconversion process and also enhanced its cellular uptake and enables high quality imaging through NIR laser scanning microscopy. Further, this nanoconjugate defines dose-dependent cytotoxicity to oral squamous cell carcinoma (OSCC) without damaging healthy cells and thus can serve as a promising agent for theranostic purpose. As it is well known, that FR is overexpressed in numerous cancers and thus it proves to have clinical significance in development of FR targeted theranostic agent (Cheung et al. 2016). In this context, Sun et al. demonstrated the synthesis and bioimaging application of three different kinds of folate targeted UCNPs i.e. UCNP-FA:UCNP-Er-FA, UCNP-Tm-FA, and UCNP-Er,Tm-FA (Sun et al. 2014). Result showed that these NPs exhibit excellent targeting to cancerous cells and also have good biocompatibility and low toxicity. UCNPs-FA imaging agents are found to be water-dispersible and viability assay suggests that it displayed excellent in vitro biocompatibility. Histological and hematological studies revealed no apparent toxicity to living system (Kunming mice). All these properties proposed that UCNPs conjugates act as potential fluorescent contrast agent. Gureyv et al. demonstrated the combined therapy using UCNPs conjugated to two different therapeutic agents: beta-emitting radionuclide yttrium-90 (<sup>90</sup>Y), fractionally substituting yttrium in UCNPs and exotoxin A fragment which exerts its toxic effect to cancerous cells (Fig. 9) (Guryev et al. 2018). <sup>90</sup>Y (Beta emitter), is enclosed in UCNPs core and have short half-life of 63 h and high linear density of radiation energy transfer, which allows the radiation impact localization within several millimeters and further leads to reduced side effects (Audi et al. 2003; Lyra et al. 2013). Theranostic complex UCNP-R-T (R, radioactive; T, toxic) contains targeting biomolecule, which is specific to HER2 overexpressing cells and belongs to the class of designed ankyrin repeat protein (DARPin) (Sokolova et al. 2016). This hybrid complex was further tested on HER2 receptor overexpressing human breast carcinoma cells, SK-BR-3 cells and immunodeficient mice, with HER2 positive xenograft tumor. Nanocomplexes were intratumorally administered into mice to reduce the systemic toxic effect. Result showed that at a single exposure of 15 µg/g, UCNPs exhibits > 40% of TGI effect. Ionizing radiation was absorbed maximally on day 5 after UCNP-R-T administration, which corresponds to the highest TGI observed at same time point. The photophysical properties of UCNPs further enable the background free imaging of UCNP-R-T distributed in animals and cells. Photoluminescence data further suggest that the half-life of UCNP-R-T

**Table 4** Quantum dots application in cancer detection and therapy

Nanosystem	Target molecule	Cell line/animals	Application	Result	References
Silica NPs-carbon dots	FA	HeLa, MCF7, A549 and L929 cells	Fluorescence image-guided drug carrier	Nanohybrid exhibits superior performance for imaging-guided drug delivery to FR overexpressing HeLa cells	Zhao et al. (2019c)
GQDs	Herceptin, DOX	SK-BR-3 and MDA-MB-231 cells	Antitumor activity and intracellular trafficking	Cellular uptake and antitumor activity was enhanced in HER2 overexpressing cells	Ko et al. (2019)
QDs/IONPs	Biotinylation site (BS), docking domain	MCF-7, MDA-MB-231, SKBR3 cells	Early cancer detection, hyperthermia	Hybrid peptide detects the HER2/ <i>neu</i> -positive breast cancer cells due to QDs-fluorescence and destroyed as a result of the IONPs-mediated hyperthermia	Chang et al. (2019a)
AgGa <sub>x</sub> In <sub>(1-x)</sub> S <sub>2</sub> (AGIS) QDs	Low-density lipoprotein (LDL)	NCM-460 cells	Photoluminescence probe 3D imaging of cancer stem cells	Nanoprobe shows receptor-mediated internalization. Utilized in 3D imaging of cancer cells	Song et al. (2019)
GQDs	FA	SKOV3, MDA-MB-231, MCF7 cells	Intracellular trafficking	Nanoprobe shows receptor-mediated internalization. Utilized in 3D imaging of cancer cells	Zhang et al. (2019)
Nitrogen-doped carbon dots (N-CD)	DOX	HeLa cells	Fluorescence imaging	N-CDs exhibited high quality single- and two-photon fluorescence in high depth (18 μm), enabling the N-CDs based real-time monitor of endocytosis, intracellular distribution, and release of drugs. Study indicate the IFE fluorescence strategy can expediently detect β-glucuronidase in living cells	Gong et al. (2019)
Nitrogen-doped GQDs	FA	MKN 45, HT 29 and MCF7 cells.	Fluorescent imaging of cancer cells	Nanoprobe showed enhanced uptake in FR overexpressing cells	Soleymani et al. (2018)

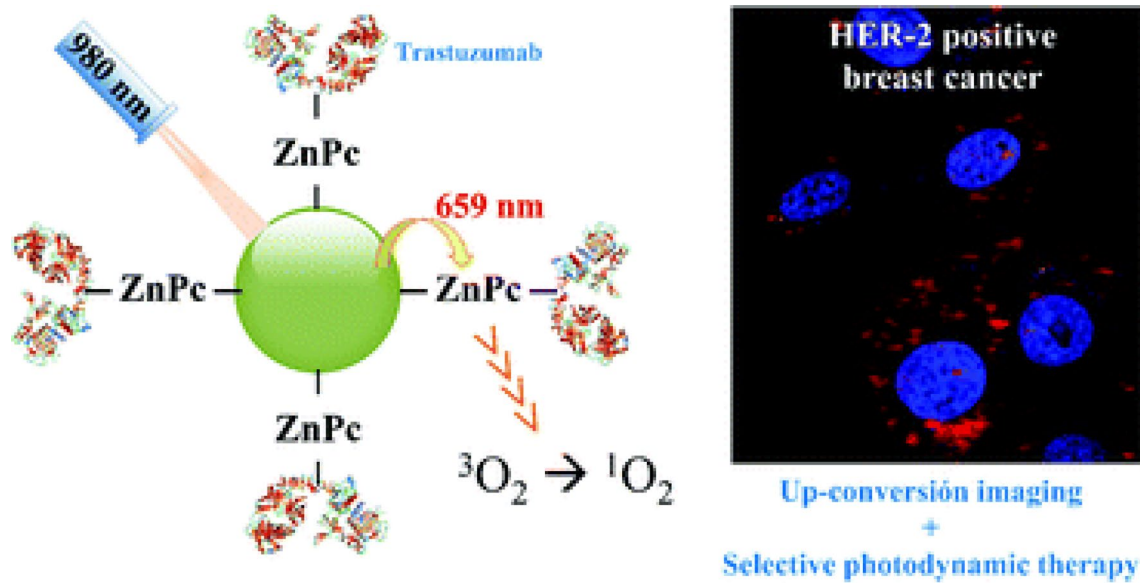
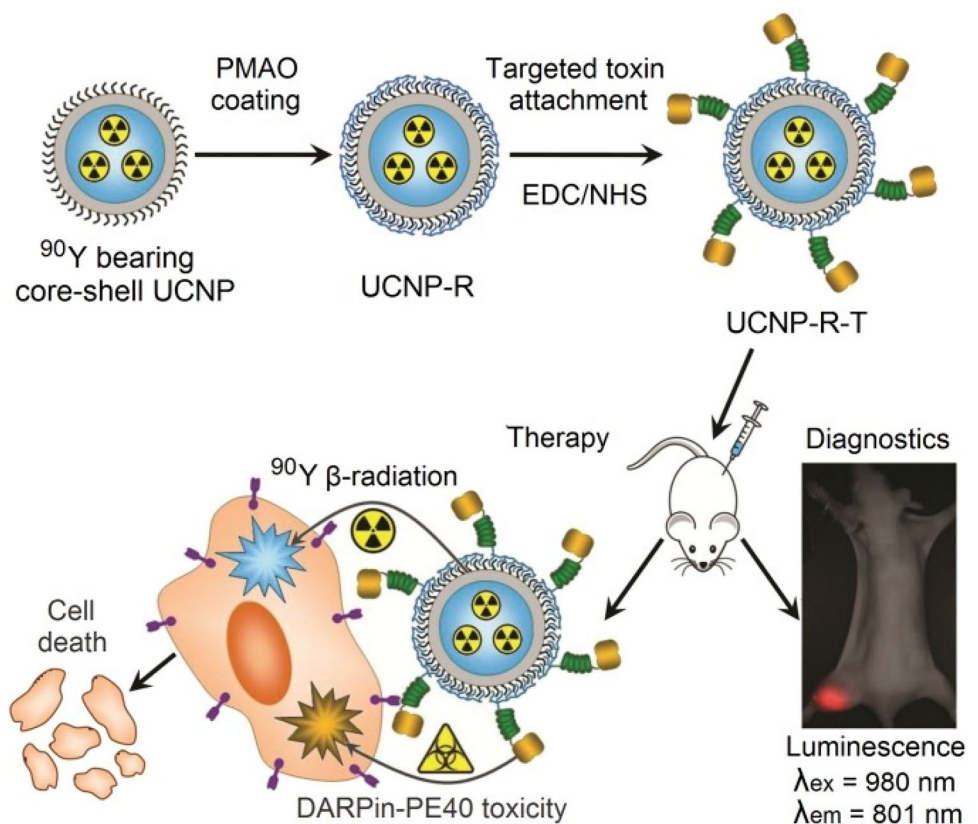


**Fig. 8** Schematic showing application of UCNP nanoconjugate for tracking and Photodynamic therapy of HER2 positive breast cancer cells. Reprinted with permission from Gracia et al. 2018, *Nanoscale*. Copyright 2019, Royal Society of Chemistry (Ramirez-Garcia et al. 2018)

**Fig. 9** Assembly and mode of action of the hybrid biofunctional nanocomplex UCNP-R-T. *R* radioactive, *T* toxic; targeting module, targeted toxin DARPin-PE40. (Magnification:  $\times 2$ ). Reprinted from Guryev et al. (2018), 115(39):9690–9695 (Guryev et al. 2018)



in tumor node was recorded as 150 h (~6 days). Synergistic effect of UCNP-R-T increased to about 2200-fold in comparison to UCNP-R or T alone. Due to their high upconversion luminescence (UCL) efficiency,  $\text{Yb}^{3+}$  sensitized UCNPs

under 980 nm excitation, has been used in photo-triggered theranostic application. However, water and biological tissues strongly absorb the 980 nm light which induces damage due to the overheating effect. To overcome this limitation,



**Table 5** Upconversion nanoparticles based cancer detection and therapy

Nanosystem	Target molecule/drug	Cell line/animals	Application	Result	References
$\text{Yb}^{3+}$ and $\text{Tm}^{3+}$ co-doped $\text{NaGdF}_4$ UCNPs	ZnO nanodots and polypyrrole	HeLa cells	PDT and PTT	Synergistic effect of PTT and PDT give rise to excellent anti-tumor efficacy. Generate ROS and hyperthermia upon 980 nm light irradiation	Cai et al. (2018)
$\beta\text{-NaGdF}_4\text{:Yb,Er,X\%Lu}$ ( $X=0, 1, 2.5, 4, 6, 7.5$ ) UCNPs	–	HepG2 cells	Dual mode imaging as UCL/CT nanoprobe	$\text{NH}_2$ -PEGylated- $\text{NaGdF}_4\text{:Yb,Er,X\%Lu}$ NPs exhibited low cytotoxicity, high biocompatibility, and remarkably enhanced contrast performance in <i>in vitro</i> UCL and <i>in vivo</i> CT imaging	Liu et al. (2018b)
$\text{NaYF}_4\text{:Yb}^{3+}, \text{Er}^{3+}$ UCNPs	RGD, DOX	MCF-7 cells	PDT and cascade chemotherapy	Upon NIR irradiation, the light emission from UCNPs could excite photosensitizer to produce ROS for PDT along with the activation of caspase-3, which further cleaved DEVD peptide to release DOX within tumor cells, thus accomplishing anti-tumor activity	Zhao et al. (2017)
$\text{NaYF}_4$ UCNPs	Rhodamine B	A549 Cells	Imaging and PDT	980 nm NIR irradiation induces green light emissions for cell imaging, and 660 nm red light emission was excited for activating photosensitizers to generate singlet oxygen, which could be exploited directly to kill cancer cells	Wang et al. (2016)
$\text{GO/ZnFe}_2\text{O}_4$ /UCNPs		HeLa cells and Female Kunming mice	UCL, CT, MRI, PAT	Based on Fenton reaction that $\text{ZnFe}_2\text{O}_4$ NPs react with excessive $\text{H}_2\text{O}_2$ in tumor microenvironment to produce toxic $\cdot\text{OH}$ radicals, an excellent anticancer efficiency has been achieved	Bi et al. (2018)

Table 5 (continued)

Nanosystem	Target molecule/drug	Cell line/animals	Application	Result	References
NaYF <sub>4</sub> :Yb,Er@NaGdF <sub>4</sub> UCNP <sub>s</sub>	Anti-EpCAM and Mitoxantrone	BEL-7404 tumor-bearing mice and RAW 264.7 macrophages	Chemotherapy and PDT	Micelles exhibit good biocompatibility, high specificity to cancerous cells and superior fluorescent/magnetic properties in vitro. In vivo results demonstrate that the targeted micelles exhibited much better MR/UCL imaging qualities	Han et al. (2018)
NaLuF <sub>4</sub> :Er <sup>3+</sup> , Yb <sup>3+</sup> with nanographene oxide (NGO)		Mouse breast cancer cells (4T1) cells and BALB/c mice	Upconversion fluorescence imaging and PDT	Excellent biocompatibility and low toxicity of the novel UCNPs@NGO nanoplatform were demonstrated by cytotoxicity assays, and the nanoplatform showed great potential to serve as a UCL imaging probe for animal whole-body with high contrast. In addition, PTT treatments of UCNPs@NGO on tumor cells both in vitro and in vivo indicate prominent performances of the NP in inhibiting tumor growth	Li et al. (2018a)

800 nm light excitation has been served as an ideal candidate due to its less absorption by water molecules (Li et al. 2018b). In this context, Li et al. demonstrated the 800 nm driven NaErF<sub>4</sub>@NaLuF<sub>4</sub> UCNPs for multimodality imaging and NIR triggered PDT. Result showed that optimal ~5 nm shell thickness can balance the UCL enhancement and attenuation of energy transfer efficiency from Er<sup>3+</sup> towards photosensitizer, for production of singlet oxygen for PDT under 800 nm excitation. Under 800 nm NIR laser irradiation, NaErF<sub>4</sub>@NaLuF<sub>4</sub> UCNPs exhibit significant increase in cytotoxic effect which corresponds to decrease in cell viability (~26%) in comparison of cells which are not irradiated, thus confirming the NIR induced cancer cell killing ability. In vivo study clearly suggest no pathological changes in kidney, lung, liver, heart, and spleen. Additionally, as obtained UCNPs can also found its application in UCL, CT imaging and high field T2 MRI. In the proposed system, Er<sup>3+</sup> ions T2 relaxation rate can be utilized as MRI contrast agent whereas, Lu<sup>3+</sup> ions provide high X-ray attenuation (slope 23.86) for CT imaging. Thus, this approach provides new 800 nm driven NMs to reduce the thermal side effect during cancer therapy. Table 5 summarizes some more UCNPs application in cancer therapy. Thus, from all of the above reported literature it can be concluded that UCNPs attached to different ligands can be successfully utilized in the diagnosis and therapy of cancer.

## Conclusion and future outlooks

This review presents the recent developments in the field of nanomedicine for their use in cancer imaging and diagnosis. Due to their unique properties, these NPs can revolutionize the various imaging modalities i.e. AuNPs and IONPs serve as a contrast probe in CT imaging and MRI respectively, whereas, QDs and UCNPs can be employed as a probe in fluorescence imaging. Combination of more than one imaging probe can circumvent the drawback of each other and thus can reduce the chance of misdiagnosis. As discussed in this article, several chemotherapeutic agents can be loaded or conjugated with the nanoplatfroms to achieve theranostic application. In biological environment, behavior of NPs is governed by several factors like delivery route, particle size, surface coating, and targeting molecules, which occasionally limit their application as nanomedicine. Due to the paucity in clinically approved therapies, full potential of nanomedicine has yet to be realized. Attention should be paid to the biosafety of these materials due to the possible side effects on human health and environment. Unlike, in vivo imaging studies where NPs have to be administered systemically in body, nano-biosensors can be utilized in in vitro application and thus do not invoke the possibility of complications arises due to toxicity and biodistribution. These nano-biosensors

are proved to be more efficient and sensitive detection tool than conventional methods like ELISA. However, further clinical development and corroborations are required for sensitive and early detection of cancer.

Efficacy of NMs depends on numerous aspects like targeted delivery of NPs to tumor site, EPR effect, tumor heterogeneity, tumor microenvironment and metastasis prevention, nano-bio interaction, and host-tumor immunological crosstalk. While considering the future entities like RNA, CRISPR components and immunotherapy, role of microbiome and metabolic inferences also play important insight into the synthesis of nanomedicine. In spite of all challenges, prevailing views suggest that nanomedicine has potential to revolutionize the not only oncological landscape but also medicine in a broader way. In upcoming decades, advances and understanding in the field of nanotechnological innovations will elevate the nanomedicine specifically NPs based targeted drug delivery from bench to clinical approaches in the treatment of cancer and several other diseases.

**Funding** This study is funded by Liaocheng University (Grant No. 318051901).

## Compliance with ethical standards

**Conflict of interest** Author declares no conflict of interest.

## References

- Abdelhamid AS, Zayed DG, Helmy MW, Ebrahim SM, Bahey-El-Din M, Zein-El-Dein EA, El-Gizawy SA, Elzoghby AO (2018) Lactoferrin-tagged quantum dots-based theranostic nanocapsules for combined COX-2 inhibitor/herbal therapy of breast cancer. *Nanomedicine (Lond)* 13(20):2637–2656. <https://doi.org/10.2217/nmm-2018-0196>
- Akram M, Iqbal M, Daniyal M, Khan AU (2017) Awareness and current knowledge of breast cancer. *Biol Res* 50(1):33. <https://doi.org/10.1186/s40659-017-0140-9>
- Amer MH (2014) Gene therapy for cancer: present status and future perspective. *Mol Cell Ther* 2:27. <https://doi.org/10.1186/2052-8426-2-27>
- Audi G, Bersillon O, Blachot J, Wapstra A (2003) The NUBASE evaluation of nuclear and decay properties. *Nuclear Phys A* 729(1):3–128
- Bansal S, Singh J, Kumari U, Kaur IP, Barnwal RP, Kumar R, Singh S, Singh G, Chatterjee M (2019) Development of biosurfactant-based graphene quantum dot conjugate as a novel and fluorescent theranostic tool for cancer. *Int J Nanomed* 14:809–818. <https://doi.org/10.2147/IJN.S188552>
- Barlas FB, Aydinoglu E, Arslan M, Timur S, Yagci Y (2019) Gold nanoparticle conjugated poly(p-phenylene-β-cyclodextrin)-graft-poly(ethylene glycol) for theranostic applications. *J Appl Polym Sci* 136(12):47250. <https://doi.org/10.1002/app.47250>
- Bi H, He F, Dai Y, Xu J, Dong Y, Yang D, Gai S, Li L, Li C, Yang P (2018) Quad-model imaging-guided high-efficiency phototherapy based on upconversion nanoparticles and ZnFe<sub>2</sub>O<sub>4</sub> Integrated graphene oxide. *Inorg Chem* 57(16):9988–9998. <https://doi.org/10.1021/acs.inorgchem.8b01159>

- Bray F, Jemal A, Grey N, Ferlay J, Forman D (2012) Global cancer transitions according to the Human Development Index (2008–2030): a population-based study. *Lancet Oncol* 13(8):790–801. [https://doi.org/10.1016/S1470-2045\(12\)70211-5](https://doi.org/10.1016/S1470-2045(12)70211-5)
- Cai Q, Xu J, Yang D, Dai Y, Yang G, Zhong C, Gai S, He F, Yang P (2018) Polypyrrole-coated UCNPs@mSiO<sub>2</sub>@ZnO nanocomposite for combined photodynamic and photothermal therapy. *J Mater Chem B* 6(48):8148–8162. <https://doi.org/10.1039/C8TB02407C>
- Cao Y, Dong H, Yang Z, Zhong X, Chen Y, Dai W, Zhang X (2017) Aptamer-conjugated graphene quantum dots/porphyrin derivative theranostic agent for intracellular cancer-related microRNA detection and fluorescence-guided photothermal/photodynamic synergetic therapy. *ACS Appl Mater Interfaces* 9(1):159–166. <https://doi.org/10.1021/acsami.6b13150>
- Casalini P, Iorio MV, Galmozzi E, Menard S (2004) Role of HER receptors family in development and differentiation. *J Cell Physiol* 200(3):343–350. <https://doi.org/10.1002/jcp.20007>
- Chan MS, Tam DY, Dai Z, Liu LS, Ho JW, Chan ML, Xu D, Wong MS, Tin C, Lo PK (2016) Mitochondrial delivery of therapeutic agents by amphiphilic DNA nanocarriers. *Small* 12(6):770–781. <https://doi.org/10.1002/sml.201503051>
- Chang C-H, Tsai IC, Chiang C-J, Chao Y-P (2019a) A theranostic approach to breast cancer by a quantum dots- and magnetic nanoparticles-conjugated peptide. *J Taiwan Inst Chem Eng* 97:88–95. <https://doi.org/10.1016/j.jtice.2019.02.013>
- Chang J, Zhang A, Huang Z, Chen Y, Zhang Q, Cui D (2019b) Monodisperse Au@Ag core-shell nanoprobe with ultrasensitive SERS-activity for rapid identification and Raman imaging of living cancer cells. *Talanta* 198:45–54. <https://doi.org/10.1016/j.talanta.2019.01.085>
- Chaudhary A, Dwivedi C, Gupta A, Nandi CK (2015) One pot synthesis of doxorubicin loaded gold nanoparticles for sustained drug release. *RSC Adv* 5(118):97330–97334. <https://doi.org/10.1039/C5RA12892G>
- Chen H, Zhen Z, Todd T, Chu PK, Xie J (2013) Nanoparticles for improving cancer diagnosis. *Mater Sci Eng R Rep* 74(3):35–69. <https://doi.org/10.1016/j.mser.2013.03.001>
- Chen G, Qiu H, Prasad PN, Chen X (2014) Upconversion nanoparticles: design, nanochemistry, and applications in theranostics. *Chem Rev* 114(10):5161–5214. <https://doi.org/10.1021/cr400425h>
- Chen C, Zhou S, Cai Y, Tang F (2017a) Nucleic acid aptamer application in diagnosis and therapy of colorectal cancer based on cell-SELEX technology. *NPJ Precis Oncol* 1(1):37. <https://doi.org/10.1038/s41698-017-0041-y>
- Chen F, Gao W, Qiu X, Zhang H, Liu L, Liao P, Fu W, Luo Y (2017b) Graphene quantum dots in biomedical applications: recent advances and future challenges. *Front Lab Med* 1(4):192–199. <https://doi.org/10.1016/j.flm.2017.12.006>
- Chen J, Li X, Zhao X, Wu Q, Zhu H, Mao Z, Gao C (2018) Doxorubicin-conjugated pH-responsive gold nanorods for combined photothermal therapy and chemotherapy of cancer. *Bioact Mater* 3(3):347–354. <https://doi.org/10.1016/j.bioactmat.2018.05.003>
- Chen X, Han W, Zhao X, Tang W, Wang F (2019) Epirubicin-loaded marine carrageenan oligosaccharide capped gold nanoparticle system for pH-triggered anticancer drug release. *Sci Rep* 9(1):6754. <https://doi.org/10.1038/s41598-019-43106-9>
- Cheng Y, Cheng H, Jiang C, Qiu X, Wang K, Huan W, Yuan A, Wu J, Hu Y (2015) Perfluorocarbon nanoparticles enhance reactive oxygen levels and tumour growth inhibition in photodynamic therapy. *Nat Commun* 6:8785. <https://doi.org/10.1038/ncomm9785>
- Cheung A, Bax HJ, Josephs DH, Ilieva KM, Pellizzari G, Opzoomer J, Bloomfield J, Fittall M, Grigoriadis A, Figini M, Canevari S, Spicer JF, Tutt AN, Karagiannis SN (2016) Targeting folate receptor alpha for cancer treatment. *Oncotarget* 7(32):52553–52574. <https://doi.org/10.18632/oncotarget.9651>
- Chung US, Kim JH, Kim B, Kim E, Jang WD, Koh WG (2016) Dendrimer porphyrin-coated gold nanoshells for the synergistic combination of photodynamic and photothermal therapy. *Chem Commun (Camb)* 52(6):1258–1261. <https://doi.org/10.1039/c5cc09149g>
- Cryer AM, Thorley AJ (2019) Nanotechnology in the diagnosis and treatment of lung cancer. *Pharmacol Ther* 198:189–205. <https://doi.org/10.1016/j.pharmthera.2019.02.010>
- De M, Ghosh S, Sen T, Shadab M, Banerjee I, Basu S, Ali N (2018) A novel therapeutic strategy for cancer using phosphatidylserine targeting stearylamine-bearing cationic liposomes. *Mol Ther Nucleic Acids* 10:9–27. <https://doi.org/10.1016/j.omtn.2017.10.019>
- Dean L (2015) Trastuzumab (herceptin) therapy and ERBB2 (HER2) genotype. In: *Medical Genetics Summaries* [Internet]. National Center for Biotechnology Information (US)
- Deng H, Dai F, Ma G, Zhang X (2015) Theranostic gold nanomicelles made from biocompatible comb-like polymers for thermochemotherapy and multifunctional imaging with rapid clearance. *Adv Mater* 27(24):3645–3653. <https://doi.org/10.1002/adma.201501420>
- Dey C, Ghosh A, Ahir M, Ghosh A, Goswami MM (2018) Improvement of anticancer drug release by cobalt ferrite magnetic nanoparticles through combined pH and temperature responsive technique. *ChemPhysChem* 19(21):2872–2878. <https://doi.org/10.1002/cphc.201800535>
- Diamantis N, Banerji U (2016) Antibody-drug conjugates—an emerging class of cancer treatment. *Br J Cancer* 114(4):362–367. <https://doi.org/10.1038/bjc.2015.435>
- Dong H, Sun LD, Yan CH (2015) Energy transfer in lanthanide upconversion studies for extended optical applications. *Chem Soc Rev* 44(6):1608–1634. <https://doi.org/10.1039/c4cs00188e>
- Du AW, Stenzel MH (2014) Drug carriers for the delivery of therapeutic peptides. *Biomacromol* 15(4):1097–1114. <https://doi.org/10.1021/bm500169p>
- Elbially NS, Fathy MM, Al-Wafi R, Darwesh R, Abdel-Dayem UA, Aldhahri M, Noorwali A, Al-Ghamdi AA (2019) Multifunctional magnetic-gold nanoparticles for efficient combined targeted drug delivery and interstitial photothermal therapy. *Int J Pharm* 554:256–263. <https://doi.org/10.1016/j.ijpharm.2018.11.021>
- Eleftheriadis T, Pissas G, Liakopoulos V, Stefanidis I (2016) Cytochrome c as a potentially clinical useful marker of mitochondrial and cellular damage. *Front Immunol* 7:279. <https://doi.org/10.3389/fimmu.2016.00279>
- Fang M, Dai-Wen Li PY (2016) Quantum dots for cancer diagnosis. *Biomed Nanomater*. <https://doi.org/10.1002/9783527694396.ch8>
- Farooq MU, Novosad V, Rozhkova EA, Wali H, Ali A, Fateh AA, Neogi PB, Neogi A, Wang Z (2018) Gold nanoparticles-enabled efficient dual delivery of anticancer therapeutics to HeLa cells. *Sci Rep* 8(1):2907. <https://doi.org/10.1038/s41598-018-21331-y>
- Feng T, Ai X, An G, Yang P, Zhao Y (2016) Charge-convertible carbon dots for imaging-guided drug delivery with enhanced in vivo cancer therapeutic efficiency. *ACS Nano* 10(4):4410–4420. <https://doi.org/10.1021/acsnano.6b00043>
- Feng J, Huang P, Shi S, Deng KY, Wu FY (2017) Colorimetric detection of glutathione in cells based on peroxidase-like activity of gold nanoclusters: a promising powerful tool for identifying cancer cells. *Anal Chim Acta* 967:64–69. <https://doi.org/10.1016/j.aca.2017.02.025>
- Fernandes AR, Jesus J, Martins P, Figueiredo S, Rosa D, Martins LM, Corvo ML, Carvalho MC, Costa PM, Baptista PV (2017) Multifunctional gold-nanoparticles: a nanovectorization tool for the targeted delivery of novel chemotherapeutic agents. *J Control Release* 245:52–61. <https://doi.org/10.1016/j.jconrel.2016.11.021>



- Ferrara N (2002) VEGF and the quest for tumour angiogenesis factors. *Nat Rev Cancer* 2(10):795–803. <https://doi.org/10.1038/nrc909>
- Fu S, Wang S, Zhang X, Qi A, Liu Z, Yu X, Chen C, Li L (2017) Structural effect of Fe<sub>3</sub>O<sub>4</sub> nanoparticles on peroxidase-like activity for cancer therapy. *Colloids Surf B Biointerfaces* 154:239–245. <https://doi.org/10.1016/j.colsurfb.2017.03.038>
- Fukaminato T, Ishida S, Métivier R (2018) Photochromic fluorophores at the molecular and nanoparticle levels: fundamentals and applications of diarylethenes. *NPG Asia Mater* 10(9):859–881. <https://doi.org/10.1038/s41427-018-0075-9>
- Galle PR, Foerster F, Kudo M, Chan SL, Llovet JM, Qin S, Schelman W, Chintharlapalli S, Abada P, Sherman M, Zhu AX (2019) Biology and significance of alpha-fetoprotein in hepatocellular carcinoma. *Liver Int.* <https://doi.org/10.1111/liv.14223>
- Gao C, Deng ZJ, Peng D, Jin YS, Ma Y, Li YY, Zhu YK, Xi JZ, Tian J, Dai ZF, Li CH, Liang XL (2016) Near-infrared dye-loaded magnetic nanoparticles as photoacoustic contrast agent for enhanced tumor imaging. *Cancer Biol Med* 13(3):349–359. <https://doi.org/10.20892/j.issn.2095-3941.2016.0048>
- Gardner A, Ruffell B (2016) Dendritic cells and cancer immunity. *Trends Immunol* 37(12):855–865. <https://doi.org/10.1016/j.it.2016.09.006>
- Ge J, Jia Q, Liu W, Guo L, Liu Q, Lan M, Zhang H, Meng X, Wang P (2015) Red-emissive carbon dots for fluorescent, photoacoustic, and thermal theranostics in living mice. *Adv Mater* 27(28):4169–4177. <https://doi.org/10.1002/adma.201500323>
- Gellerman G, Baskin S, Galia L, Gilad Y, Firer MA (2013) Drug resistance to chlorambucil in murine B-cell leukemic cells is overcome by its conjugation to a targeting peptide. *Anticancer Drugs* 24(2):112–119. <https://doi.org/10.1097/CAD.0b013e32835bb17a>
- Gong P, Sun L, Wang F, Liu X, Yan Z, Wang M, Zhang L, Tian Z, Liu Z, You J (2019) Highly fluorescent N-doped carbon dots with two-photon emission for ultrasensitive detection of tumor marker and visual monitor anticancer drug loading and delivery. *Chem Eng J* 356:994–1002. <https://doi.org/10.1016/j.cej.2018.09.100>
- Greish K (2010) Enhanced permeability and retention (EPR) effect for anticancer nanomedicine drug targeting. *Methods Mol Biol* 624:25–37. [https://doi.org/10.1007/978-1-60761-609-2\\_3](https://doi.org/10.1007/978-1-60761-609-2_3)
- Guo J, Rahme K, He Y, Li LL, Holmes JD, O'Driscoll CM (2017) Gold nanoparticles enlighten the future of cancer theranostics. *Int J Nanomed* 12:6131–6152. <https://doi.org/10.2147/IJN.S140772>
- Guryev EL, Volodina NO, Shilyagina NY, Gudkov SV, Balalaeva IV, Volovetskiy AB, Lyubeshkin AV, Sen AV, Ermilov SA, Vodeenev VA, Petrov RV, Zvyagin AV, Alferov ZI, Deyev SM (2018) Radioactive ((90)Y) upconversion nanoparticles conjugated with recombinant targeted toxin for synergistic nanotheranostics of cancer. *Proc Natl Acad Sci USA* 115(39):9690–9695. <https://doi.org/10.1073/pnas.1809258115>
- Hale SJM, Perrins RD, Garci AC, Pace A, Peral U, Patel KR, Robinson A, Williams P, Ding Y, Saito G, Rodriguez MA, Perera I, Barrientos A, Conlon K, Damment S, Porter J, Coulter T (2019) DM1 loaded ultrasmall gold nanoparticles display significant efficacy and improved tolerability in murine models of hepatocellular carcinoma. *Bioconjugate Chem* 30(3):703–713. <https://doi.org/10.1021/acs.bioconjchem.8b00873>
- Han Y, An Y, Jia G, Wang X, He C, Ding Y, Tang Q (2018) Theranostic micelles based on upconversion nanoparticles for dual-modality imaging and photodynamic therapy in hepatocellular carcinoma. *Nanoscale* 10(14):6511–6523. <https://doi.org/10.1039/C7NR09717D>
- He J, Dong J, Hu Y, Li G, Hu Y (2019) Design of Raman tag-bridged core-shell Au@Cu<sub>3</sub>(BTC)<sub>2</sub> nanoparticles for Raman imaging and synergistic chemo-photothermal therapy. *Nanoscale* 11(13):6089–6100. <https://doi.org/10.1039/c9nr00041k>
- Herreros-Villanueva M, Bujanda L (2016) Glypican-1 in exosomes as biomarker for early detection of pancreatic cancer. *Ann Transl Med* 4(4):64. <https://doi.org/10.3978/j.issn.2305-5839.2015.10.39>
- Hlapiš N, Motaung TE, Liganiso LZ, Oluwafemi OS, Songca SP (2019) Encapsulation of gold nanorods with porphyrins for the potential treatment of cancer and bacterial diseases: a critical review. *Bioinorg Chem Appl* 2019:7147128. <https://doi.org/10.1155/2019/7147128>
- Ho CM, Chang SF, Hsiao CC, Chien TY, Shih DTB (2012) Isolation and characterization of stromal progenitor cells from ascites of patients with epithelial ovarian adenocarcinoma. *J Biomed Sci.* <https://doi.org/10.1186/1423-0127-19-23>
- Hu D, Sheng Z, Fang S, Wang Y, Gao D, Zhang P, Gong P, Ma Y, Cai L (2014) Folate receptor-targeting gold nanoclusters as fluorescence enzyme mimetic nanoprobe for tumor molecular colocalization diagnosis. *Theranostics* 4(2):142–153. <https://doi.org/10.7150/thno.7266>
- Hu J, Liu MH, Li Y, Tang B, Zhang CY (2018) Simultaneous sensitive detection of multiple DNA glycosylases from lung cancer cells at the single-molecule level. *Chem Sci* 9(3):712–720. <https://doi.org/10.1039/c7sc04296e>
- Huang P, Lin J, Wang X, Wang Z, Zhang C, He M, Wang K, Chen F, Li Z, Shen G, Cui D, Chen X (2012) Light-triggered theranostics based on photosensitizer-conjugated carbon dots for simultaneous enhanced-fluorescence imaging and photodynamic therapy. *Adv Mater* 24(37):5104–5110. <https://doi.org/10.1002/adma.201200650>
- Hynes RO (2002) Integrins: bidirectional, allosteric signaling machines. *Cell* 110(6):673–687
- Imanparast A, Bakhshizadeh M, Salek R, Sazgarnia A (2018) Pegylated hollow gold-mitoxantrone nanoparticles combining photodynamic therapy and chemotherapy of cancer cells. *Photodiagn Photodyn Ther* 23:295–305. <https://doi.org/10.1016/j.pdpdt.2018.07.011>
- Israeli RS, Powell CT, Fair WR, Heston WD (1993) Molecular cloning of a complementary DNA encoding a prostate-specific membrane antigen. *Cancer Res* 53(2):227–230
- Jie G, Gao X, Ge J, Li C (2019) Multifunctional DNA nanocage with CdTe quantum dots for fluorescence detection of human 8-oxoG DNA glycosylase 1 and doxorubicin delivery to cancer cells. *Mikrochim Acta* 186(2):85. <https://doi.org/10.1007/s00604-018-3199-2>
- Kale SS, Burga RA, Sweeney EE, Zun Z, Sze RW, Tuesca A, Subramony JA, Fernandes R (2017) Composite iron oxide-Prussian blue nanoparticles for magnetically guided T1-weighted magnetic resonance imaging and photothermal therapy of tumors. *Int J Nanomed* 12:6413–6424. <https://doi.org/10.2147/IJN.S144515>
- Kalimuthu K, Lubin BC, Bazylevich A, Gellerman G, Shpilberg O, Luboshits G, Firer MA (2018) Gold nanoparticles stabilize peptide-drug-conjugates for sustained targeted drug delivery to cancer cells. *J Nanobiotechnol* 16(1):34. <https://doi.org/10.1186/s12951-018-0362-1>
- Key J, Cooper C, Kim AY, Dhawan D, Knapp DW, Kim K, Park JH, Choi K, Kwon IC, Park K, Leary JF (2012) In vivo NIRF and MR dual-modality imaging using glycol chitosan nanoparticles. *J Control Release* 163(2):249–255. <https://doi.org/10.1016/j.jconrel.2012.07.038>
- Khan SN, Lal SK, Kumar P, Khan AU (2010) Effect of mitoxantrone on proliferation dynamics and cell-cycle progression. *Biosci Rep* 30(6):375–381. <https://doi.org/10.1042/BSR20090119>
- Kim Y, Lee S, Kim D, Noh K, Oh KS, Cho S, Choi E, Kim K-p, Huh KM (2018) Preparation and characterization of poly (ethylene glycol)-doxorubicin/SPION magnetic nanoparticles for cancer therapy. *POLYMER-KOREA* 42(6):1059–1067
- Kim JS, Jang JY, Cheon HJ, Cho S, Jang IS, Yu BJ, Kim MI (2019) Co(3)O(4)/Au hybrid nanostructures as efficient peroxidase

- mimics for colorimetric biosensing. *J Nanosci Nanotechnol* 19(10):6696–6702. <https://doi.org/10.1166/jnn.2019.17098>
- Ko NR, Hong SH, Nafiujjaman M, An SY, Revuri V, Lee SJ, Kwon IK, Lee Y-k, Oh SJ (2019) Glutathione-responsive PEGylated GQD-based nanomaterials for diagnosis and treatment of breast cancer. *J Ind Eng Chem* 71:301–307. <https://doi.org/10.1016/j.jiec.2018.11.039>
- Kobayashi M, Sawada K, Kimura T (2017) Potential of integrin inhibitors for treating ovarian cancer: a literature review. *Cancers (Basel)*. <https://doi.org/10.3390/cancers9070083>
- Kou J, Dou D, Yang L (2017) Porphyrin photosensitizers in photodynamic therapy and its applications. *Oncotarget* 8(46):81591–81603. <https://doi.org/10.18632/oncotarget.20189>
- Lai X, Zhao H, Zhang Y, Guo K, Xu Y, Chen S, Zhang J (2018) Intranasal delivery of copper oxide nanoparticles induces pulmonary toxicity and fibrosis in C57BL/6 mice. *Sci Rep* 8(1):4499. <https://doi.org/10.1038/s41598-018-22556-7>
- Lee H, Lee JH, Kim J, Mun JH, Chung J, Koo H, Kim C, Yun SH, Hahn SK (2016) Hyaluronate-gold nanorod/DR5 antibody complex for noninvasive theranosis of skin cancer. *ACS Appl Mater Interfaces* 8(47):32202–32210. <https://doi.org/10.1021/acsami.6b11319>
- Lee S, Lee C, Park S, Lim K, Kim SS, Kim JO, Lee ES, Oh KT, Choi HG, Youn YS (2018) Facile fabrication of highly photothermal-effective albumin-assisted gold nanoclusters for treating breast cancer. *Int J Pharm* 553(1–2):363–374. <https://doi.org/10.1016/j.ijpharm.2018.10.063>
- Li P, Yan Y, Chen B, Zhang P, Wang S, Zhou J, Fan H, Wang Y, Huang X (2018a) Lanthanide-doped upconversion nanoparticles complexed with nano-oxide graphene used for upconversion fluorescence imaging and photothermal therapy. *Biomater Sci* 6(4):877–884. <https://doi.org/10.1039/c7bm01113j>
- Li Q, Li X, Zhang L, Zuo J, Zhang Y, Liu X, Tu L, Xue B, Chang Y, Kong X (2018b) An 800 nm driven NaErF<sub>4</sub>@NaLuF<sub>4</sub> upconversion platform for multimodality imaging and photodynamic therapy. *Nanoscale* 10(26):12356–12363. <https://doi.org/10.1039/c8nr00446c>
- Li K, Hong E, Wang B, Wang Z, Zhang L, Hu R, Wang B (2019a) Advances in the application of upconversion nanoparticles for detecting and treating cancers. *Photodiagn Photodyn Ther* 25:177–192. <https://doi.org/10.1016/j.pdpdt.2018.12.007>
- Li W, Xue B, Shi K, Qu Y, Chu B, Qian Z (2019b) Magnetic iron oxide nanoparticles/10-hydroxy camptothecin co-loaded nanogel for enhanced photothermal-chemo therapy. *Appl Mater Today* 14:84–95. <https://doi.org/10.1016/j.apmt.2018.11.008>
- Liu J, Yu M, Zhou C, Yang S, Ning X, Zheng J (2013) Passive tumor targeting of renal-clearable luminescent gold nanoparticles: long tumor retention and fast normal tissue clearance. *J Am Chem Soc* 135(13):4978–4981. <https://doi.org/10.1021/ja401612x>
- Liu Y, Ma D, Ji C (2015) Zinc fingers and homeoboxes family in human diseases. *Cancer Gene Ther* 22(5):223–226. <https://doi.org/10.1038/cgt.2015.16>
- Liu H, Zhang J, Chen X, Du XS, Zhang JL, Liu G, Zhang WG (2016a) Application of iron oxide nanoparticles in glioma imaging and therapy: from bench to bedside. *Nanoscale* 8(15):7808–7826. <https://doi.org/10.1039/c6nr00147e>
- Liu J, Yang Y, Zhu W, Yi X, Dong Z, Xu X, Chen M, Yang K, Lu G, Jiang L, Liu Z (2016b) Nanoscale metal-organic frameworks for combined photodynamic and radiation therapy in cancer treatment. *Biomaterials* 97:1–9. <https://doi.org/10.1016/j.biomaterials.2016.04.034>
- Liu L, Li E, Luo L, Zhao S, Li F, Wang J, Luo J, Zhao Z (2017) PSCA regulates IL-6 expression through p38/NF-kappaB signaling in prostate cancer. *Prostate* 77(14):1389–1400. <https://doi.org/10.1002/pros.23399>
- Liu HN, Guo NN, Wang TT, Guo WW, Lin MT, Huang-Fu MY, Vakili MR, Xu WH, Chen JJ, Wei QC, Han M, Lavasanifar A, Gao JQ (2018a) Mitochondrial targeted doxorubicin-triphenylphosphonium delivered by hyaluronic acid modified and pH responsive nanocarriers to breast tumor: in vitro and in vivo studies. *Mol Pharm* 15(3):882–891. <https://doi.org/10.1021/acs.molpharmaceut.7b00793>
- Liu M, Shi Z, Wang X, Zhang Y, Mo X, Jiang R, Liu Z, Fan L, Ma CG, Shi F (2018b) Simultaneous enhancement of red upconversion luminescence and CT contrast of NaGdF<sub>4</sub>:Yb, Er nanoparticles via Lu(3+) doping. *Nanoscale* 10(43):20279–20288. <https://doi.org/10.1039/c8nr06968a>
- Lo YL, Lo PC, Chiu CC, Wang LF (2015) Folic acid linked chondroitin sulfate-polyethyleneimine copolymer based gene delivery system. *J Biomed Nanotechnol* 11(8):1385–1400
- Loo JF, Lau PM, Kong SK, Ho HP (2017) An assay using localized surface plasmon resonance and gold nanorods functionalized with aptamers to sense the cytochrome-c released from apoptotic cancer cells for anti-cancer drug effect determination. *Micromachines (Basel)*. <https://doi.org/10.3390/mi8110338>
- Lugert S, Unterwiesing H, Muhlberger M, Janko C, Draack S, Ludwig F, Eberbeck D, Alexiou C, Friedrich RP (2019) Cellular effects of paclitaxel-loaded iron oxide nanoparticles on breast cancer using different 2D and 3D cell culture models. *Int J Nanomedicine* 14:161–180. <https://doi.org/10.2147/IJN.S187886>
- Luo L, Liu C, He T, Zeng L, Xing J, Xia Y, Pan Y, Gong C, Wu A (2018) Engineered fluorescent carbon dots as promising immune adjuvants to efficiently enhance cancer immunotherapy. *Nanoscale* 10(46):22035–22043. <https://doi.org/10.1039/c8nr07252c>
- Lyer S, Singh R, Tietze R, Alexiou C (2015) Magnetic nanoparticles for magnetic drug targeting. *Biomed Tech (Berl)* 60(5):465–475. <https://doi.org/10.1515/bmt-2015-0049>
- Lyra ME, Andreou M, Georgantzoglou A, Kordolaimi S, Lagopati N, Ploussi A, Salvara A-L, Vamvakas I (2013) Radionuclides used in nuclear medicine therapy—from production to dosimetry. *Curr Med Imaging Rev* 9(1):51–75
- Maji SK, Mandal AK, Nguyen KT, Borah P, Zhao Y (2015) Cancer cell detection and therapeutics using peroxidase-active nanohybrid of gold nanoparticle-loaded mesoporous silica-coated graphene. *ACS Appl Mater Interfaces* 7(18):9807–9816. <https://doi.org/10.1021/acsami.5b01758>
- Mancic L, Djukic-Vukovic A, Dinic I, Nikolic MG, Rabasovic MD, Krmpot AJ, Costa A, Trisic D, Lazarevic M, Mojovic L, Milosevic O (2018) NIR photo-driven upconversion in NaYF<sub>4</sub>:Yb, Er/PLGA particles for in vitro bioimaging of cancer cells. *Mater Sci Eng C Mater Biol Appl* 91:597–605. <https://doi.org/10.1016/j.msec.2018.05.081>
- Marchetti C, Palaia I, Giorgini M, De Medici C, Iadarola R, Vertechy L, Domenici L, Di Donato V, Tomao F, Muzii L, Benedetti Panici S (2014) Targeted drug delivery via folate receptors in recurrent ovarian cancer: a review. *Onco Targets Ther* 7:1223–1236. <https://doi.org/10.2147/OTT.S40947>
- Mbatha LS, Singh M (2019) Starburst poly(amidoamine) dendrimer grafted gold nanoparticles as a scaffold for folic acid-targeted plasmid dna delivery in vitro. *J Nanosci Nanotechnol* 19(4):1959–1970. <https://doi.org/10.1166/jnn.2019.15798>
- Mehra NK, Mishra V, Jain NK (2013) Receptor-based targeting of therapeutics. *Ther Deliv* 4(3):369–394. <https://doi.org/10.4155/tde.13.6>
- Mitra RN, Doshi M, Zhang X, Tyus JC, Bengtsson N, Fletcher S, Page BD, Turkson J, Gesquiere AJ, Gunning PT, Walter GA, Santra S (2012) An activatable multimodal/multifunctional nanoprobe for direct imaging of intracellular drug delivery. *Biomaterials* 33(5):1500–1508. <https://doi.org/10.1016/j.biomaterials.2011.10.068>

- Mundy GR (2002) Metastasis to bone: causes, consequences and therapeutic opportunities. *Nat Rev Cancer* 2(8):584–593. <https://doi.org/10.1038/nrc867>
- Nakamura H, Nishimura T (2017) History, molecular features, and clinical importance of conventional serum biomarkers in lung cancer. *Surg Today* 47(9):1037–1059. <https://doi.org/10.1007/s00595-017-1477-y>
- Nasrollahi F, Koh YR, Chen P, Varshosaz J, Khodadadi AA, Lim S (2019) Targeting graphene quantum dots to epidermal growth factor receptor for delivery of cisplatin and cellular imaging. *Mater Sci Eng C Mater Biol Appl* 94:247–257. <https://doi.org/10.1016/j.msec.2018.09.020>
- Olson WC, Heston WD, Rajasekaran AK (2007) Clinical trials of cancer therapies targeting prostate-specific membrane antigen. *Rev Recent Clin Trials* 2(3):182–190
- Pandey S, Thakur M, Mewada A, Anjarlekar D, Mishra N, Sharon M (2013) Carbon dots functionalized gold nanorod mediated delivery of doxorubicin: tri-functional nano-worms for drug delivery, photothermal therapy and bioimaging. *J Mater Chem B* 1(38):4972–4982. <https://doi.org/10.1039/C3TB20761G>
- Pandey V, Gajbhiye KR, Soni V (2015) Lactoferrin-appended solid lipid nanoparticles of paclitaxel for effective management of bronchogenic carcinoma. *Drug Deliv* 22(2):199–205. <https://doi.org/10.3109/10717544.2013.877100>
- Pang B, Yang X, Xia Y (2016) Putting gold nanocages to work for optical imaging, controlled release and cancer theranostics. *Nanomedicine (Lond)* 11(13):1715–1728. <https://doi.org/10.2217/nmm-2016-0109>
- Park MH, Hong JE, Hwang CJ, Choi M, Choi JS, An YJ, Son DJ, Hong JT (2016) Synergistic inhibitory effect of cetuximab and tectochrysin on human colon cancer cell growth via inhibition of EGFR signal. *Arch Pharmacol Res* 39(5):721–729. <https://doi.org/10.1007/s12272-016-0735-7>
- Peng Y, Wang Z, Liu W, Zhang H, Zuo W, Tang H, Chen F, Wang B (2015) Size- and shape-dependent peroxidase-like catalytic activity of MnFe<sub>2</sub>O<sub>4</sub> Nanoparticles and their applications in highly efficient colorimetric detection of target cancer cells. *Dalton Trans* 44(28):12871–12877. <https://doi.org/10.1039/c5dt01585e>
- Perez-Ortiz M, Zapata-Urzuca C, Acosta GA, Alvarez-Lueje A, Albericio F, Kogan MJ (2017) Gold nanoparticles as an efficient drug delivery system for GLP-1 peptides. *Colloids Surf B Biointerfaces* 158:25–32. <https://doi.org/10.1016/j.colsurfb.2017.06.015>
- Perfezou M, Turner A, Merkoci A (2012) Cancer detection using nanoparticle-based sensors. *Chem Soc Rev* 41(7):2606–2622. <https://doi.org/10.1039/c1cs15134g>
- Piawah S, Venook AP (2019) Targeted therapy for colorectal cancer metastases: a review of current methods of molecularly targeted therapy and the use of tumor biomarkers in the treatment of metastatic colorectal cancer. *Cancer*. <https://doi.org/10.1002/ncr.32163>
- Pierrat P, Wang R, Kereselidze D, Lux M, Didier P, Kichler A, Pons F, Lebeau L (2015) Efficient in vitro and in vivo pulmonary delivery of nucleic acid by carbon dot-based nanocarriers. *Biomaterials* 51:290–302. <https://doi.org/10.1016/j.biomaterials.2015.02.017>
- Plan Sangnier A, Aufaure R, Motte L, Wilhelm C, Guenin E, Lalatonne Y (2018) Hybrid Au@alendronate nanoparticles as dual chemophotothermal agent for combined cancer treatment. *Beilstein J Nanotechnol* 9:2947–2952. <https://doi.org/10.3762/bjnano.9.273>
- Polasek M, Yang Y, Schuhle DT, Yaseen MA, Kim YR, Sung YS, Guimaraes AR, Caravan P (2017) Molecular MR imaging of fibrosis in a mouse model of pancreatic cancer. *Sci Rep* 7(1):8114. <https://doi.org/10.1038/s41598-017-08838-6>
- Poon KA, Flagella K, Beyer J, Tibbitts J, Kaur S, Saad O, Yi JH, Girish S, Dybdal N, Reynolds T (2013) Preclinical safety profile of trastuzumab emtansine (T-DM1): mechanism of action of its cytotoxic component retained with improved tolerability. *Toxicol Appl Pharmacol* 273(2):298–313. <https://doi.org/10.1016/j.taap.2013.09.003>
- Poonia M, Ramalingam K, Goyal S, Sidhu SK (2017) Nanotechnology in oral cancer: a comprehensive review. *J Oral Maxillofac Pathol* 21(3):407–414. [https://doi.org/10.4103/jomfp.JOMFP\\_29\\_17](https://doi.org/10.4103/jomfp.JOMFP_29_17)
- Pucci M, Lauriola M (2019) Chapter 18—resistance to EGFR targeting treatments in colorectal cancer. In: Dammacco F, Silvestris F (eds) *Oncogenomics*. Academic Press, Cambridge, pp 257–269. <https://doi.org/10.1016/B978-0-12-811785-9.00018-1>
- Qiu W, Chen R, Chen X, Zhang H, Song L, Cui W, Zhang J, Ye D, Zhang Y, Wang Z (2018) Oridonin-loaded and GPC1-targeted gold nanoparticles for multimodal imaging and therapy in pancreatic cancer. *Int J Nanomed* 13:6809–6827. <https://doi.org/10.2147/IJN.S177993>
- Ramezanzadeh E, Sadri K, Momenzadeh M, Dolat E, Sazgarnia A (2018) Evaluation of EGFR-targeted gold/gold sulfide (GGS) nanoparticles as a theranostic agent in photothermal therapy. *Natur Res Express* 5(12):125401. <https://doi.org/10.1088/2053-1591/aadfa0>
- Ramirez-Garcia G, Panikar SS, Lopez-Luke T, Piazza V, Honorato-Colin MA, Camacho-Villegas T, Hernandez-Gutierrez R, De la Rosa E (2018) An immunoconjugated up-conversion nanocomplex for selective imaging and photodynamic therapy against HER2-positive breast cancer. *Nanoscale* 10(21):10154–10165. <https://doi.org/10.1039/c8nr01512k>
- Ren Q-Q, Bai L-Y, Zhang X-S, Ma Z-Y, Liu B, Zhao Y-D, Cao Y-C (2015) Preparation, modification, and application of hollow gold nanospheres. *J Nanomater* 2015:7. <https://doi.org/10.1155/2015/534070>
- Scherer RL, McIntyre JO, Matrisian LM (2008) Imaging matrix metalloproteinases in cancer. *Cancer Metastasis Rev* 27(4):679–690. <https://doi.org/10.1007/s10555-008-9152-9>
- Sebastian S, Settleman J, Reshkin SJ, Azzariti A, Bellizzi A, Paradiso A (2006) The complexity of targeting EGFR signalling in cancer: from expression to turnover. *Biochim Biophys Acta* 1766(1):120–139. <https://doi.org/10.1016/j.bbcan.2006.06.001>
- Shen C, Wang X, Zheng Z, Gao C, Chen X, Zhao S, Dai Z (2019) Doxorubicin and indocyanine green loaded superparamagnetic iron oxide nanoparticles with PEGylated phospholipid coating for magnetic resonance with fluorescence imaging and chemotherapy of glioma. *Int J Nanomed* 14:101–117. <https://doi.org/10.2147/IJN.S173954>
- Shepard HM, Phillips GL, Thanos CD, Feldmann M (2017) Developments in therapy with monoclonal antibodies and related proteins. *Clin Med (Lond)* 17(3):220–232. <https://doi.org/10.7861/clinmedicine.17-3-220>
- Shindo Y, Hazama S, Tsunedomi R, Suzuki N, Nagano H (2019) Novel biomarkers for personalized cancer immunotherapy. *Cancers (Basel)*. <https://doi.org/10.3390/cancers11091223>
- Sokolova E, Proshkina G, Kutova O, Shilova O, Ryabova A, Schulga A, Stremovskiy O, Zdobnova T, Balalaeva I, Deyev S (2016) Recombinant targeted toxin based on HER2-specific DARPIn possesses a strong selective cytotoxic effect in vitro and a potent antitumor activity in vivo. *J Control Release* 233:48–56. <https://doi.org/10.1016/j.jconrel.2016.05.020>
- Soleymani J, Hasanzadeh M, Somi MH, Ozkan SA, Jouyban A (2018) Targeting and sensing of some cancer cells using folate bioreceptor functionalized nitrogen-doped graphene quantum dots. *Int J Biol Macromol* 118:1021–1034. <https://doi.org/10.1016/j.ijbmac.2018.06.183>
- Song S, Chong Y, Fu H, Ning X, Shen H, Zhang Z (2018) HP-beta-CD functionalized Fe<sub>3</sub>O<sub>4</sub>/CNPs-based theranostic nanoplatform for pH/NIR responsive drug release and MR/NIRFL imaging-guided synergetic chemo/photothermal therapy of tumor. *ACS Appl*



- Mater Interfaces 10(40):33867–33878. <https://doi.org/10.1021/acsami.8b09999>
- Song JL, Zhang Y, Dai YW, Hu JH, Zhu LX, Xu XL, Yu Y, Li H, Yao B, Zhou HX (2019) Polyelectrolyte-mediated nontoxic AgGaxIn1-xS2 QDs/low-density lipoprotein nanoprobe for selective 3d fluorescence imaging of cancer stem cells. ACS Appl Mater Interfaces 11(10):9884–9892. <https://doi.org/10.1021/acsami.9b00121>
- Sonker N, Bajpai J, Bajpai AK (2018) Magnetically responsive release of 5-FU from superparamagnetic egg albumin coated iron oxide core-shell nanoparticles. J Drug Deliv Sci Technol 47:240–253. <https://doi.org/10.1016/j.jddst.2018.07.021>
- Stambuk N, Konjevoda P, Turcic P, Sosic H, Aralica G, Babic D, Seiwert H, Kastelan Z, Kujundzic RN, Wardega P, Zutelija JB, Gracanin AG, Gabricevic M (2019) Targeting tumor markers with antisense peptides: an example of human prostate specific antigen. Int J Mol Sci. <https://doi.org/10.3390/ijms20092090>
- Stellavato A, Corsuto L, D'Agostino A, La Gatta A, Diana P, Bernini P, De Rosa M, Schiraldi C (2016) Hyaluronan hybrid cooperative complexes as a novel frontier for cellular bioprocesses reactivation. PLoS One 11(10):e0163510. <https://doi.org/10.1371/journal.pone.0163510>
- Strebhardt K, Ullrich A (2008) Paul Ehrlich's magic bullet concept: 100 years of progress. Nat Rev Cancer 8(6):473–480. <https://doi.org/10.1038/nrc2394>
- Sun L, Wei Z, Chen H, Liu J, Guo J, Cao M, Wen T, Shi L (2014) Folic acid-functionalized up-conversion nanoparticles: toxicity studies in vivo and in vitro and targeted imaging applications. Nanoscale 6(15):8878–8883. <https://doi.org/10.1039/c4nr02312a>
- Sun S, Zhang L, Jiang K, Wu A, Lin H (2016) Toward high-efficient red emissive carbon dots: facile preparation, unique properties, and applications as multifunctional theranostic agents. Chem Mater 28(23):8659–8668. <https://doi.org/10.1021/acs.chemmater.6b03695>
- Tao Y, Lin Y, Huang Z, Ren J, Qu X (2013) Incorporating graphene oxide and gold nanoclusters: a synergistic catalyst with surprisingly high peroxidase-like activity over a broad pH range and its application for cancer cell detection. Adv Mater 25(18):2594–2599. <https://doi.org/10.1002/adma.201204419>
- Tao Y, Li M, Kim B, Auguste DT (2017) Incorporating gold nanoclusters and target-directed liposomes as a synergistic amplified colorimetric sensor for HER2-positive breast cancer cell detection. Theranostics 7(4):899–911. <https://doi.org/10.7150/thno.17927>
- Teraoka S, Kakei Y, Akashi M, Iwata E, Hasegawa T, Miyawaki D, Sasaki R, Komori T (2018) Gold nanoparticles enhance X-ray irradiation-induced apoptosis in head and neck squamous cell carcinoma in vitro. Biomed Rep 9(5):415–420. <https://doi.org/10.3892/br.2018.1142>
- Tian J, Ding L, Xu HJ, Shen Z, Ju H, Jia L, Bao L, Yu JS (2013) Cell-specific and pH-activatable rubryrin-loaded nanoparticles for highly selective near-infrared photodynamic therapy against cancer. J Am Chem Soc 135(50):18850–18858. <https://doi.org/10.1021/ja408286k>
- Tseng SH, Chou MY, Chu IM (2015) Cetuximab-conjugated iron oxide nanoparticles for cancer imaging and therapy. Int J Nanomed 10:3663–3685. <https://doi.org/10.2147/IJN.S80134>
- Turnis ME, Rooney CM (2010) Enhancement of dendritic cells as vaccines for cancer. Immunotherapy 2(6):847–862. <https://doi.org/10.2217/imt.10.56>
- Verhoven B, Schlegel RA, Williamson P (1995) Mechanisms of phosphatidylserine exposure, a phagocyte recognition signal, on apoptotic T lymphocytes. J Exp Med 182(5):1597–1601. <https://doi.org/10.1084/jem.182.5.1597>
- Viel A, Bruselles A, Meccia E, Fornasarig M, Quaia M, Canzonieri V, Policicchio E, Urso ED, Agostini M, Genuardi M, Lucci-Cordisco E, Venesio T, Martayan A, Diodoro MG, Sanchez-Mete L, Stigliano V, Mazzei F, Grasso F, Giuliani A, Baiocchi M, Maestro R, Giannini G, Tartaglia M, Alexandrov LB, Bignami M (2017) A specific mutational signature associated with DNA 8-oxoguanine persistence in MUTYH-defective colorectal cancer. EBioMedicine 20:39–49. <https://doi.org/10.1016/j.ebiom.2017.04.022>
- Villalobos P, Wistuba II (2017) Lung cancer biomarkers. Hematol Oncol Clin North Am 31(1):13–29. <https://doi.org/10.1016/j.hoc.2016.08.006>
- Vu-Quang H, Vinding MS, Nielsen T, Ullisch MG, Nielsen NC, Nguyen DT, Kjems J (2019) Pluronic F127-folate coated super paramagnetic iron oxide nanoparticles as contrast agent for cancer diagnosis in magnetic resonance imaging. Polymers (Basel). <https://doi.org/10.3390/polym11040743>
- Wang C, Cheng L, Liu Z (2013a) Upconversion nanoparticles for photodynamic therapy and other cancer therapeutics. Theranostics 3(5):317–330. <https://doi.org/10.7150/thno.5284>
- Wang P, Nie X, Wang Y, Li Y, Ge C, Zhang L, Wang L, Bai R, Chen Z, Zhao Y, Chen C (2013b) Multiwall carbon nanotubes mediate macrophage activation and promote pulmonary fibrosis through TGF-beta/Smad signaling pathway. Small 9(22):3799–3811. <https://doi.org/10.1002/sml.201300607>
- Wang H, Han RL, Yang LM, Shi JH, Liu ZJ, Hu Y, Wang Y, Liu SJ, Gan Y (2016) Design and synthesis of core-shell-shell upconversion nanoparticles for NIR-induced drug release, photodynamic therapy, and cell imaging. ACS Appl Mater Interfaces 8(7):4416–4423. <https://doi.org/10.1021/acsami.5b11197>
- Weaver O, Leung JWT (2018) Biomarkers and imaging of breast cancer. AJR Am J Roentgenol 210(2):271–278. <https://doi.org/10.2214/AJR.17.18708>
- Weitman SD, Lark RH, Coney LR, Fort DW, Frasca V, Zurawski VR Jr, Kamen BA (1992) Distribution of the folate receptor GP38 in normal and malignant cell lines and tissues. Cancer Res 52(12):3396–3401
- WHO (2018) <http://www.who.int/news-room/fact-sheets/detail/cancer>. Accessed June 2019
- Xia F, Niu J, Hong Y, Li C, Cao W, Wang L, Hou W, Liu Y, Cui D (2019) Matrix metalloproteinase 2 targeted delivery of gold nanostars decorated with IR-780 iodide for dual-modal imaging and enhanced photothermal/photodynamic therapy. Acta Biomater 89:289–299. <https://doi.org/10.1016/j.actbio.2019.03.008>
- Xiang D, Zheng C, Zhou SF, Qiao S, Tran PH, Pu C, Li Y, Kong L, Kouzani AZ, Lin J, Liu K, Li L, Shigdar S, Duan W (2015) Superior performance of aptamer in tumor penetration over antibody: implication of aptamer-based theranostics in solid tumors. Theranostics 5(10):1083–1097. <https://doi.org/10.7150/thno.11711>
- Xianyu Y, Xie Y, Wang N, Wang Z, Jiang X (2015) A dispersion-dominated chromogenic strategy for colorimetric sensing of glutathione at the nanomolar level using gold nanoparticles. Small 11(41):5510–5514. <https://doi.org/10.1002/sml.201500903>
- Xiao Z, Levy-Nissenbaum E, Alexis F, Luptak A, Teply BA, Chan JM, Shi J, Digga E, Cheng J, Langer R, Farokhzad OC (2012) Engineering of targeted nanoparticles for cancer therapy using internalizing aptamers isolated by cell-uptake selection. ACS Nano 6(1):696–704. <https://doi.org/10.1021/nn204165v>
- Yang S, You Q, Yang L, Li P, Lu Q, Wang S, Tan F, Ji Y, Li N (2019) Rodlike MSN@Au nanohybrid-modified supermolecular photosensitizer for NIRF/MSOT/CT/MR quadmodal imaging-guided photothermal/photodynamic cancer therapy. ACS Appl Mater Interfaces 11(7):6777–6788. <https://doi.org/10.1021/acsami.8b19565>
- Yiu AJ, Yiu CY (2016) Biomarkers in colorectal cancer. Anticancer Res 36(3):1093–1102
- Yousoufian H, Hicklin DJ, Rowinsky EK (2007) Review: monoclonal antibodies to the vascular endothelial growth factor receptor-2 in



- cancer therapy. *Clin Cancer Res* 13(18 Pt 2):5544s–5548s. <https://doi.org/10.1158/1078-0432.CCR-07-1107>
- Yuan R, Rao T, Cheng F, Yu WM, Ruan Y, Zhang XB, Larre S (2018) Quantum dot-based fluorescent probes for targeted imaging of the EJ human bladder urothelial cancer cell line. *Exp Ther Med* 16(6):4779–4783. <https://doi.org/10.3892/etm.2018.6805>
- Zarschler K, Rocks L, Licciardello N, Boselli L, Polo E, Garcia KP, De Cola L, Stephan H, Dawson KA (2016) Ultrasmall inorganic nanoparticles: state-of-the-art and perspectives for biomedical applications. *Nanomedicine* 12(6):1663–1701. <https://doi.org/10.1016/j.nano.2016.02.019>
- Zhang M, Kim HS, Jin T, Woo J, Piao YJ, Moon WK (2017) Near-infrared photothermal therapy using anti-EGFR-gold nanorod conjugates for triple negative breast cancer. *Oncotarget* 8(49):86566–86575. <https://doi.org/10.18632/oncotarget.21243>
- Zhang M, Wang W, Wu F, Graveran K, Zhang J, Wu C (2018) Black phosphorus quantum dots gated, carbon-coated Fe<sub>3</sub>O<sub>4</sub> nanocapsules (BPQDs@ss-Fe<sub>3</sub>O<sub>4</sub>@C) with low premature release could enable imaging-guided cancer combination therapy. *Chemistry* 24(49):12890–12901. <https://doi.org/10.1002/chem.201801085>
- Zhang Q, Deng S, Liu J, Zhong X, He J, Chen X, Feng B, Chen Y, Ostrikov K (2019) Cancer-targeting graphene quantum dots: fluorescence quantum yields, stability, and cell selectivity. *Adv Func Mater* 29(5):1805860. <https://doi.org/10.1002/adfm.201805860>
- Zhao N, Wu B, Hu X, Xing D (2017) NIR-triggered high-efficient photodynamic and chemo-cascade therapy using caspase-3 responsive functionalized upconversion nanoparticles. *Biomaterials* 141:40–49. <https://doi.org/10.1016/j.biomaterials.2017.06.031>
- Zhao C, Song X, Jin W, Wu F, Zhang Q, Zhang M, Zhou N, Shen J (2019a) Image-guided cancer therapy using aptamer-functionalized cross-linked magnetic-responsive Fe<sub>3</sub>O<sub>4</sub>@carbon nanoparticles. *Anal Chim Acta* 1056:108–116. <https://doi.org/10.1016/j.aca.2018.12.045>
- Zhao L, Li Y, Zhu J, Sun N, Song N, Xing Y, Huang H, Zhao J (2019b) Chlorotoxin peptide-functionalized polyethylenimine-entrapped gold nanoparticles for glioma SPECT/CT imaging and radionuclide therapy. *J Nanobiotechnol* 17(1):30. <https://doi.org/10.1186/s12951-019-0462-6>
- Zhao S, Sun S, Jiang K, Wang YH, Liu Y, Wu S, Li ZJ, Shu QH, Lin HW (2019c) In situ synthesis of fluorescent mesoporous silica-carbon dot nanohybrids featuring folate receptor-overexpressing cancer cell targeting and drug delivery. *Nano-Micro Lett* 11(1):13. <https://doi.org/10.1007/s40820-019-0263-3>
- Zhu DM, Xie W, Xiao YS, Suo M, Zan MH, Liao QQ, Hu XJ, Chen LB, Chen B, Wu WT, Ji LW, Huang HM, Guo SS, Zhao XZ, Liu QY, Liu W (2018) Erythrocyte membrane-coated gold nanocages for targeted photothermal and chemical cancer therapy. *Nanotechnology* 29(8):084002. <https://doi.org/10.1088/1361-6528/aa9ca1>